TAMPEREEN TEKNILLINEN YLIOPISTO
TAMPERE UNIVERSITY OF TECHNOLOGY

VILLE NIEMINEN

GENERATING GAS PHASE ODOR COMPONENTS FOR ARTIFICIAL OLFACTORY SYSTEMS

Master's Thesis

Examiners: Prof. Jukka Lekkala
M.Sc. Markus Karjalainen

Examiner and topic approved by the Faculty Council of Computing and Electrical Engineering 29th of March 2017

TIIVISTELMÄ

TAMPEREEN TEKNILLINEN YLIOPISTO
Sähkötekniikan diplomi-insinöörin tutkinto-ohjelma
VILLE NIEMINEN: KAASUMAISTEN TUOKSUKOMPONENTTIEN TUOTTAMINEN KEINOTEKOISILLE HAISTAMISJÄRJESTELMILLE
Diplomityö, 46 sivua
Syyskuu 2017
Pääaine: Biomedical engineering
Tarkastaja: professori Jukka Lekkala

Avainsanat: Olfaktometri, ionimobiliteettispektrometria, synteettinen tuoksu, elektroninen nenä

Vaikka viimevuosien tutkimukset ovat syventäneet tietämystä hajuntunnistuksesta ja sen mekanismeista, hajuaisti on edelleen ihmisen aisteista huonoiten ymmärretty. Ihmisnenässä on kymmeniä tai jopa satoja miljoonia yksittäisiä hajumolekyylejä sitovia aistimia, hajureseptoriproteiineja, joten samaan haistamistarkkuuteen pystyvän keinotekoisen nenän rakentaminen on erittäin haastavaa. Koska ihmisnenä ei ole objektiivinen sensori, hajujen tunnistamiseen ja luokitteluun laajalla skaalalla kykenevän “elektronisen nenän” kehittäminen on keinotekoisessa haistamisessa tärkeimpiä tutkimuskysymyksiä. Hajumolekyylien havaitsemisen lisäksi elektroninen nenä tarvitsee jonkin analogialtaan ihmisaivoja vastaavan osan, joka kykenee tulkitsemaan ja luokittelemaan antureilla havaitut signaalit.

Ihmisen hajuaistia tai hajujen tuottamaa psykologista reaktiota tutkittaessa tarvitaan helposti ja luotettavasti tuotettava hajustimulaatio. Hallittuja hajuntuottojärjestelmiä kutsutaan olfaktometreiksi. Tässä diplomityössä esitellään kompakti olfaktometri, joka kykenee hallitusti tuottamaan kaasumuotoisia hajukomponentteja tasaisella konsentraatiolla. Työn päätavoite oli tutkia ja todentaa, pystyykö esitelty järjestelmä suoriutumaan sille asetetuista vaatimuksista. Tuotettua kaasuvirtaa monitoroitiin kemiallisella ilmaisimella, ChemPro 100i:llä, jonka toiminta perustuu aspiraatio-ionimobilisaatiospektrometria -teknologiaan.

Esiteltyä olfaktometriä käytettiin tuottamaan synteettistä jasmiinin tuoksua käyttämällä kolmea jasmiiniöljystä löytyvää pääkomponenttia, joilla suoritettiin kokeita järjestelmän toiminnan todentamiseen. Ensimmäisessä kokeessa analysoitiin kykyä erotella ChemPro 100i -datasta eri hajukomponenteilla ja komponenttien eri konsentraatioilla toteutettuja mittauksia. Lisäksi ihmisosallistujilla toteutettiin lyhyt pilottikoe, jossa osallistujat vertailivat oikean jasmiiniöljyn ja synteettisten jasmiiniseoksien tuoksua. Tuloksista nähtiin, että esitellyllä olfaktometrilla eri konsentraatioilla tuotetut mittaukset pystyy erottamaan toisistaan. Ihmispilottikokeesta nähtiin, että ihmisnenä sekoitti oikean jasmiinin ja kol-

mea pääkomponenttia sisältäneen synteettisen jasmiinin keskenään mutta pystyi erottamaan oikean jasmiinin ja kahta pääkomponenttia sisältäneen synteettisen jasmiinin toisistaan.

ABSTRACT

TAMPERE UNIVERSITY OF TECHNOLOGY
Master's Degree Programme in Electrical engineering
VILLE NIEMINEN: GENERATING GAS PHASE ODOR COMPONENTS FOR ARTIFICIAL OLFACTORY SYSTEMS
Master of Science Thesis, 46 pages
October 2017
Major: Biomedical Engineering
Examiner: Professor Jukka Lekkala

Keywords: Olfactometry, Ion mobility spectrometry, synthetic odor, olfactometer, e-nose

Even though recent studies have led to a more refined understanding of the mechanisms related to odorant detection, the vertebrate olfactory system remains the least understood sense of the human senses. The total amount of sensing elements, olfactory receptor proteins, in the human nose is counted in tens or hundreds of millions, thus recreating this kind of complex system artificially is challenging. Human nose cannot be seen as an objective sensor, so creating an artificial olfactory system, often called electronic nose or "e-nose", which is capable to objectively and reliably classify odors in a wide range is a key research question in the field of artificial olfaction. In addition to the detection system in e-nose instruments, something analogical to human brain is needed to interpret the signals in the detecting sensors.

Production of easily controllable and measurable odor stimulus is needed when studying human olfaction, olfaction-related physiology and psychological reactions to odors. Controlled odor producing instruments are called olfactometers. In this Master Thesis, a compact olfactometer able to produce controlled continuous odor stimuli from three individual gaseous components is presented. The main objective was to study and verify if the presented system can produce gas streams with the stable concentrations of different odor components. For measuring the output air stream, the device used is a chemical detector ChemPro 100i, that is based on aspiration ion mobility spectrometry (aIMS) technology.

The presented olfactometer was used to produce synthetic jasmine scent using three main odor components from jasmine oil. Experiments were conducted to verify the functionality of our olfactometer and to analyze the capability to distinguish different odor component concentrations using the ChemPro 100i data. Further to test the functionality of our olfactometer, we run a short pilot test in which human participants compared a synthetically created scent of jasmine and the scent of real jasmine oil. Results showed that from the measurement data, different concentration sets of three components were able to be distinguished. Human pilot results showed that human nose was confused when comparing three component synthetic jasmine with real jasmine scent but could distinguish between two component synthetic jasmine and real jasmine scent.

PREFACE

This Master's thesis was carried out at the institute of Biosiences and Medical Technology (former Department of Automation Science and Engineering) in Tampere University of Technology as a part of Digital Scents (DIGITS) project which is funded by Academy of Finland. I wish to gratefully acknowledge the Academy for the funding.

Especial thanks are given to the supervisors and examiners of my thesis, professor Jukka Lekkala and M.Sc Markus Karjalainen for their guidance and support during my thesis. In addition, thanks are given to Katri Salminen and Jussi Rantala from research group for Emotions, Sociality and Computing in University of Tampere, who provided valuable insight and support regarding human perception testing.

Tampere 20.09.2017

Ville Nieminen

TABLE OF CONTENTS

ABBREVIATIONS AND NOTATIONS

AC	Adenylyl cyclase
aIMS	Aspiration ion mobility spectrometry
ATP	Adenosine triphosphate
BEA	Benzyl acetate
cAMP	Cyclic adenosine monophosphate
CIS	Cis-jasmone
CP	Conducting polymer
CV	Compensation voltage
CWA	Chemical Warfare Agent
DHS	Dynamic headspace
DIMS	Differential ion mobility spectrometry
DMA	Differential mobility analysis
DMS	Differential mobility spectrometry
DTIMS	Drift tube ion mobility spectrometry
DV	Dispersion voltage
EA	Electron affinity
FAIMS	Field asymmetric ion mobility spectrometry
GC	Gas chromatography
GDP	Guanine diphosphate
GTP	Guanine triphosphate
IMS	Ion mobility spectrometry
IND	Indole
MDA	Multivariate data analysis
MOSFET	Metal–oxide–semiconductor field-effect transistor
MS	Mass spectrometry
OBP	Odorant binding protein
OR	Olfactory receptor
OSN	Olfactory sensory neuron
PA	Proton affinity
PEEK	Polyether ether ketone
PG	Propylene glycole
SHS	Static headspace

TIC	Toxic industrial chemical
TOF	Time of flight
TW-IMS	Traveling wave ion mobility spectrometer
VOC	Volatile organic compound

.

1. INTRODUCTION

During the latest decades, research and development around odor sensing, synthetizing and creating artificial olfactory systems has become a notable field in technology. Even though recent studies have led to a more refined understanding about the mechanisms related to odorant detection, the vertebrate olfactory system remains as the least understood sense of the human senses. In vertebrate olfactory systems, the olfactory sensory neurons (OSNs) are the primary sensing cells. Human nose contains 6-10 million OSNs and each of them projects up to 50 cilia, that contain the olfactory receptor (OR) proteins, to the surface of the olfactory epithelium to sense the odor molecules.[1] This means that the total amount of sensing elements in the human nose is counted in tens or hundreds of millions, thus recreating this kind of complex system artificially is challenging.

The functioning of the human olfactory system and the resulting smell that a person identifies is dependent also on other factors than just the odor molecules entering the olfactory system. The human sensory evaluation is affected e.g. by the physiological and psychological status of the person. There is also a strong dependence between sensing taste and smell. Activating the taste buds also affect the olfactory system and vice versa, which might lead to "taste-smell confusions". A common everyday example of this is that people regularly report losing their sense of taste when their nose is blocked.[2], [3] Alterations in olfactory functions is also shown to be a marker for depression.[4]

Because the human nose cannot be seen as an objective sensor at all times, creating an artificial olfactory system, often called electronic nose or "e-nose", which is capable to objectively and reliably classify odors in a wide range is a key research question in the field of artificial olfaction. Different kinds of artificial olfactory systems have been developed for various applications. So far, the presented systems are in most cases optimized to only sense specific odors that are relevant to their specific applications and they do not provide nearly the same complexity as the natural olfactory systems. Most common current e-nose applications include explosive and drug detection [5], controlling industrial processes [6], [7] and determining food quality [8]–[10]. An important feature with e-noses is also the capability to detect odors that seem odorless for a human nose, e.g. carbon monoxide. However, this can also be seen as a non-wanted feature, depending on application. [1], [11] The whole term e-nose is also somewhat controversial as classical analytical instruments and detectors that do not provide a collective data output and are designed to detect individual components from a gas mixture are not considered e-noses in the strictest sense.[12]

For researching, testing or calibrating new e-nose -systems or sensor arrays, a reliable input signal has to be first produced to reliably verify the functioning of the system or sensor array under test. For e-noses, common input signal is volatile organic compounds (VOCs) in gaseous form. For this purpose, various methods have been proposed and produced. These kind of instruments, that can produce odor components in a precise and controlled manner, are called olfactometers. For example, Schmidt et al. have studied olfactometry and threshold levels of different scents people can identify. They presented vapor delivery device 8 (VDD8).[13] VDD8 is an olfactometer that includes syringe pump injection vapor stabilizing chamber, called vapor capacitor, optional two stage predilution with nitrogen and odor stream, and eight constant flow rate dilutors. Sommer et al. presented a mobile olfactometer that was used with fMRI-studies studying the dependence of identifying smells and activation of different regions of the brain. [14]

Molecular detection has been a large interest for a long time. Common technique for analyzing chemical compounds is gas chromatography (GC) and it is typically used in testing purity of substances or separating and detecting relative proportions of components from a mixture. GC is often also coupled with mass spectrometer (MS), instrument that measures the masses of individual molecules that are converted in to charged ions. These devices are called gas chromatography mass spectrometry (GC-MS) instruments. Ion mobility spectrometry (IMS) is a robust and sensitive method for measuring VOCs and is used especially in detecting toxic industrial chemicals (TICs), chemical warfare agents (CWAs) and explosives, but the technology is also suitable for other olfactory-related applications. IMS techniques in short work by ionizing the sample being analyzed and then observing the differences of ion mobilities between different ionic species.

In this Master's Thesis, an olfactometer able to produce odor components with controlled concentrations in gas phase was constructed. The system consists of syringe pumps, electronics and pneumatic components with three channels for three different odor components. One of the goals was to research the ability to recreate jasmine scent by only mixing two or three of its main components and to study how well both human nose and artificial olfactory system can distinguish between the created synthetic jasmine odor and real jasmine oil.

First in this thesis we get to know the basic structure, functioning and signaling of vertebrate olfactory system and how that can be related to and how it differs from artificial olfactory systems. Then we discuss the available technologies used in the current e-nose –devices and introduce some of the next generation solutions. In chapter three, the constructed compact olfactometer is introduced in detail as well as the chosen odors for the conducted measurements, some of which are displayed and discussed in chapter four. In chapter five the drawbacks and potential improvements for the olfactometer are discussed and chapter six concludes how well the objectives were achieved.

2. BACKGROUND

The roles of natural and artificial olfaction systems are unique and different. The natural olfaction system has been developed through evolution to give living creatures information about their environment (food safety, mating, detecting threats etc.) whereas artificial olfaction systems were first developed to provide information on flavor and aroma.[15] The applications for e-noses have been vastly broadened since the first developed systems to include e.g. detection of pollutants, hazardous chemicals and illnesses.[1], [12] Even as the natural and artificial olfaction systems comprise of different components, they still are analogous to each other in certain ways and have modules that are responsible for the same tasks. They both can be divided in sample delivery system, odor detection system and signal processing system leading to odor perception.[15]

In vertebrate olfaction system, the nasal cavity is responsible for the sample delivery, whereas with e-noses this can be implemented with vapor inlet tubing, pumps and related units. The working conditions between these two are vastly different as nasal cavity works under high humidity and near body temperature whereas the sensitivity of the artificial sensors to humidity and the usual requirement of high operating temperature are some of the major challenges. The detection systems in both natural and artificial olfaction systems comprise of sensing elements. In vertebrate nose, the sensing elements are tiny cilia containing OR proteins able to bind to odor molecules. In artificial systems, a broad collection of different sensors and sensor arrays with different working principles sense the odor molecules. Research with new generation biomimetic noses has started to close the gap between natural and artificial olfaction. Biomimetic noses aim to mimic the natural olfaction by using the same exact components that can be found in a natural olfactory system; ORs, odorant binding proteins (OBP) and OSNs. These components can be harvested from living creatures, such as insects. Another way to develop olfactory receptors –based sensors is to synthesize artificial peptide sequences to mimic the binding site of OR or OBP. Despite the progress, the research on the sensor development is still relatively far from achieving the sensitivity and selectivity of biological olfactory receptors.[1] That is why it is also important to continue to get a better understanding of the functioning of natural olfactory systems.

The information provided by the sensing elements is transferred to signal processing. In vertebrates, this is done by the nervous system where the brain analyzes the signals and produces a sense of smell according to the inputs. In artificial systems, the signal processing can be more or less complex, from simple signal reading and electronic fingerprint interpretation to complex machine learning solutions.

The modern GC was invented in 1952 and it has become one of the most used analytical techniques in modern chemistry. Separations of different compounds is achieved in GC

by a series of partitions between a mobile phase and a stationary liquid or solid phase. The mobile phase is a carrier gas, often an inert gas such as helium or an unreactive gas such as nitrogen. The stationary phase is a microscopic layer of the analyte, i.e. the chemical substance under analysis, inside a column (a small diameter tube, often made from glass). The rate of partitioning depends on the chemical affinity of the analyte for the stationary phase and the analyte vapor pressure, which leads to separation of compounds with different affinities.[16], [17]

IMS separates different ionic species in an electric field based on their mobilities. Ion mobility is a measure of the size-to-charge ratio of an ion. The first measurements regarding ion mobility were done already in 1897 when Ernest Rutherford measured the mobility of ions formed by x-ray ionization. During the first decades of the 20th century there was a strong interest in mobility studies and a basis in the ion kinetics theory was formed. Due to the introduction of mass spectrometry (MS), the interest in in IMS declined in 30's and 40's. The use of IMS as an analytical tool was introduced by Cohen & Karasek in 1970. Big advantage of IMS compared with most other separation methods is the operation in atmospheric pressure, which makes the instrumentation more simple and inexpensive as there is no need for vacuum pumps.[18]

IMS can be used in different ways depending on the applications; for selective detection of ions after a GC separation, for the preseparation of ions before MS or as a standalone measurement instrument. Analysis with IMS can be done in the matter of seconds which is why it is often the chosen technique in detecting compounds of interest at customs, airports and also widely in military applications.[18]

2.1 Natural olfactory system

The general structure of an olfactory system is remarkably similar across a wide range of organisms, ranging from insects to mammals. This lack of variety suggests that it represents an extremely good solution for a difficult problem. Due to the similarity, here we mainly consider the structure and mechanisms of a human olfactory system.

2.1.1 Structure of human olfactory system

The human olfactory system consists of external nose and an inner nasal cavity. The nasal cavity comprises two chambers and the cavity is covered by a mucous membrane. This membrane can be divided in two distinguishable parts, an olfactory region and a respiratory region. The mucous membrane lining the olfactory region is called olfactory epithelium, which is specialized tissue that has a crucial role in olfaction.[1] The fundamental organization of the human olfactory system is presented in Figure 1.

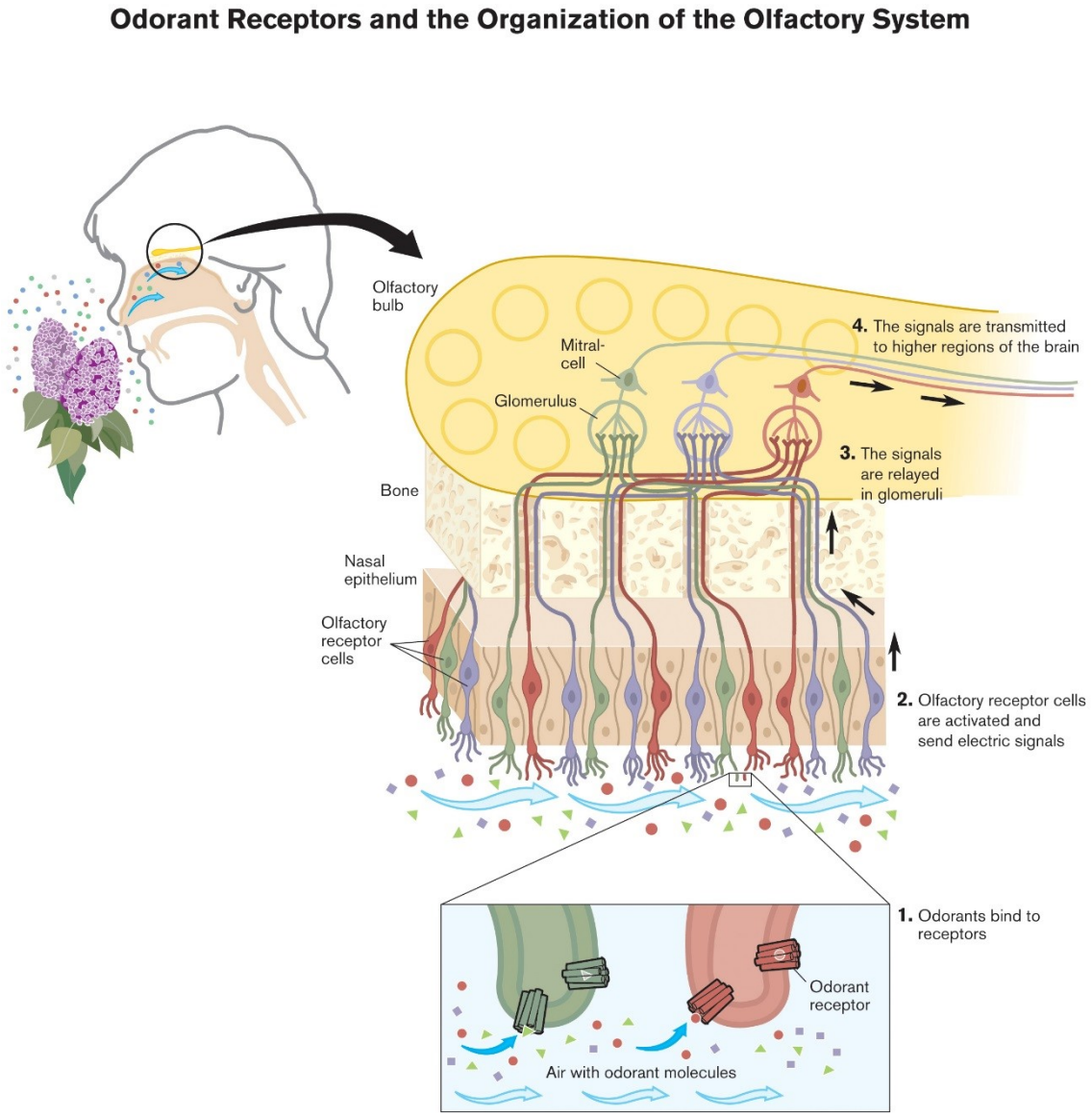

Figure 1. Structure of human olfactory system. The system activates when VOCs get in contact with odorant receptors on the surface of the nasal epithelium. Depending on what kind of VOCs are present, the associated OSNs relay a signal through glomeruli and mitral cells to higher regions of the brain. (© The Nobel Committee for Physiology or Medicine. Illustrator: Annika Röhl)

The olfactory epithelium consists of three major cell types; basal cells, supporting cells and the OSNs, also called olfactory receptor cells. The basal cells are a stem-cell population that produce new receptor cells throughout the vertebrate lifetime. Supporting cells "have numerous microvilli and secretory granules, which provide the epithelium with mucous"[1]. The main purpose of the olfactory mucosa is to provide support and protection on the surface of the epithelium for the sensory cells. The OSNs are bipolar neurons that project the very fine cilia on the surface of the epithelium. Mammalian genome contains more than 1000 different receptor types of which humans functionally express only ~400. Typically, each OSN expresses only a single receptor type and each receptor typically responds to a small subset of odorants although variance in this behavior also exists

as some receptors are responsive to a very wide range of odorants and some to only a few odorants.[19]

On the other end of each OSN is a single, unbranched axon that projects to the olfactory bulb, which is a "phylogenetically conserved brain structure"[20]. In the olfactory bulb, each axon from all the OSNs expressing the same receptor types are brought together and synapse on to one of two common points in the olfactory bulb called glomeruli. As each receptor type has two glomeruli, the number of glomeruli is double the number of different receptor types. This has been learned from rodents but the human olfactory system seems to be organized at least slightly differently as rather than the expected ~800 glomeruli, research in postmortem studies have revealed thousands of glomeruli in human olfactory bulb.[1], [19] Partly justified with this, in a recent study, McGann suggests that poor human olfaction compared to other mammals is merely a myth.[20] A key realization in comparing the olfactory performance between humans and other species has been that the selection of tested odors strongly influence the results, "presumably because different odor receptors are expressed in each species"[20].

2.1.2 Mechanisms of olfaction

The process of activating olfactory system begins when VOCs get in contact with the olfactory epithelium via the respiratory air-stream.[21] The odorants sensed in normal room conditions are low molecular weight VOCs with relatively high vapor pressure and also low water solubility and polarity.

Despite the complexity of the olfactory system, the main features of monomolecular odor processing, chemical mechanisms and signal initiation of olfactory transduction are well characterized (Fig. 2).[1], [11], [22] The OR proteins are linked to G-proteins and when the odor molecule binds to the OR protein, the protein activates and changes its shape. The activation also binds the OR proteins and G-proteins together. G-proteins consist of three subunits; alpha (α), beta (β) and gamma (γ). From these, the α-subunit is the one activated. When there is no signal (no odorants binding to the OR) the α subunit is bound to guanine diphosphate (GDP). When activation happens, GDP is replaced by guanine triphosphate (GTP). After GTP is bound to the OR, the α subunit disassociates from the other subunits and activates adenylyl cyclase (AC). In AC, the abundant intracellular molecule adenosine triphosphate (ATP) is converted to cyclic adenosine monophosphate (cAMP), which is a molecule with numerous signaling roles in cells. In OSNs the main function for cAMP is to bind to and control the ion channels. When the negative membrane potential of about -65mV is neutralized with enough positive ions flowing in the cell, the cell potential reaches threshold and generates an action potential. These action

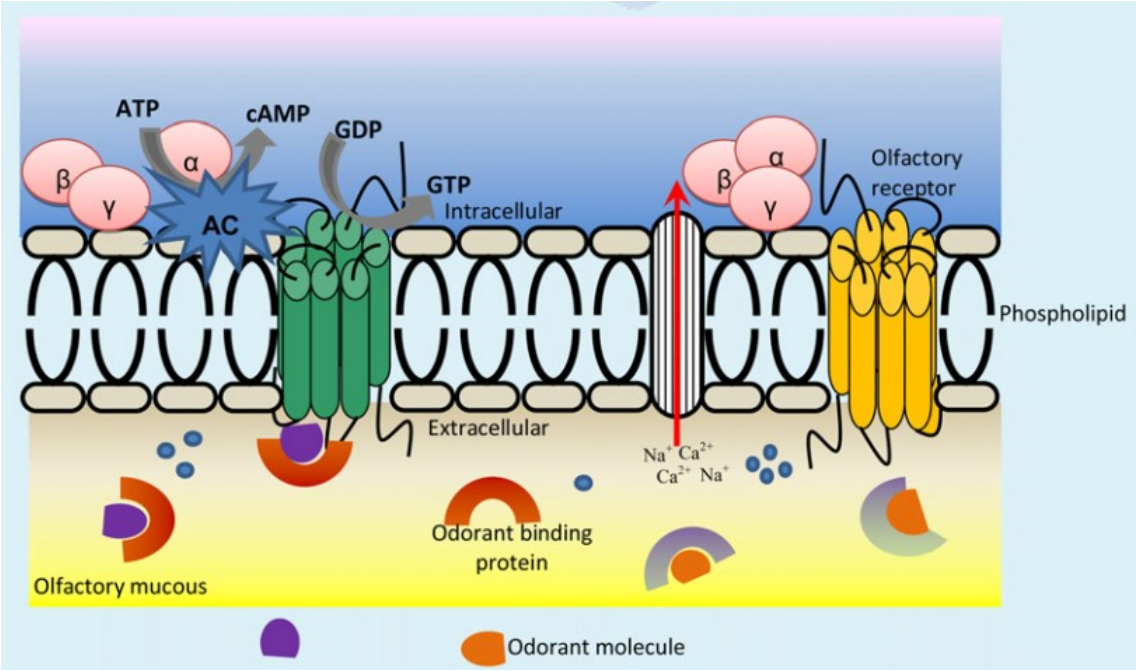

Figure 2. Chemical mechanisms in olfactory transduction. The cascading mechanism starts, when odorant is bound to OR. This activates the α-subunit of G-protein, which activates AC. In AC, ATP is converted to cAMP, that controls the ion channels and with high enough activation neutralizes the cell membrane potential and initiates an action potential.[1]

potentials are then propagated along the axons to glomeruli, from where the signals are transmitted to higher regions of brain. [1], [11], [21]

2.1.3 Olfactory coding and perception

Each OSN is typically sensitive to a small set of odorants, although there is variance in this as some receptors are responsive to only a few odorants and some to a very wide range of odorants. This receptor odorant specificity is considered the foundation of olfactory coding.[19] The brain processes signals emanating from the millions of OSNs and allows instantaneous recognition and categorization of different smells.[22]

In normal daily life, smelling single, monomolecular odors very rarely occurs. The sense of smell normally consists of the complex mixtures of volatiles that are present in the environment. In the presence of multiple odors, the interactions between the odors have a big impact on the perceived scent. In the simple case where only two odors are present in a mixture, multiple outcomes are possible (Fig. 3); a homogeneous mixture where one odor completely overshadows the other, a homogenous mixture where two odors are completely blended and the perceived odor is different to both of the source odors or a heterogeneous mixture where the odors are partially blended and/or overshadowed. It is also important to note that mixtures from the same odors can be perceived completely differently if the concentrations are tweaked. Natural odors can contain up to dozens of odor

components and the interactions are even more complex to understand or predict.[22], [23]

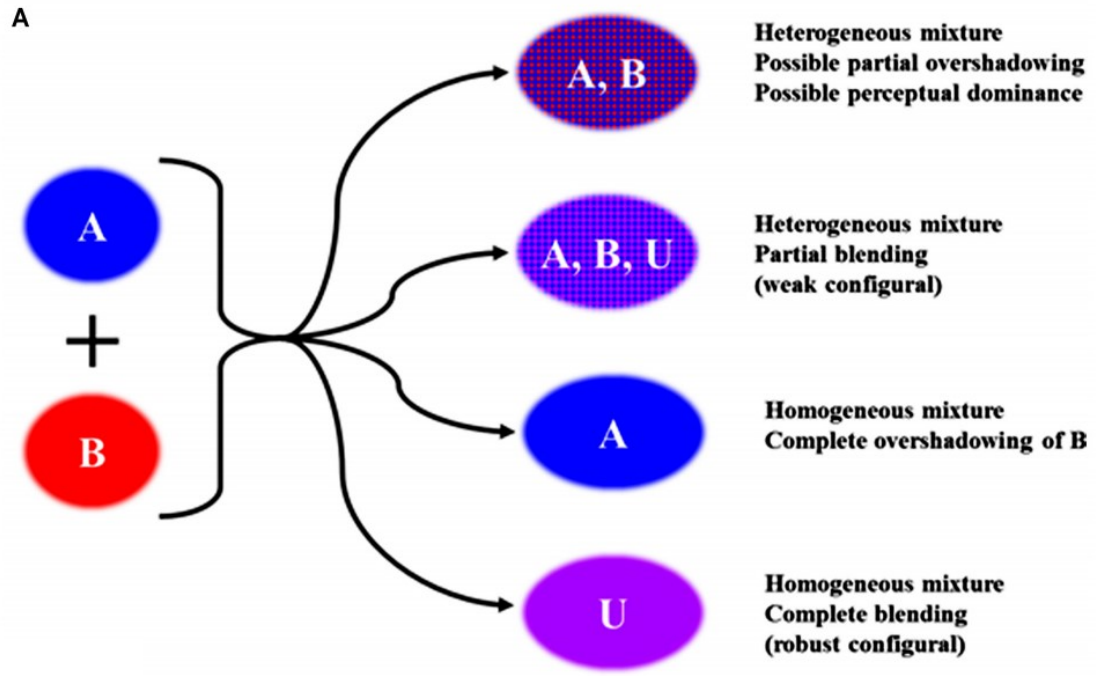

Figure 3. The possible perceived outcomes when mixing two odor components. [22]

One way to consider complex mixtures of odors is the concept of odor objects, which in other words can be seen as the ability of an olfactory system to capture complex chemical information as a whole. An aspect supporting the theory of odor objects is the number of different odorants that can be distinguished from complex odor mixtures. Studies have shown that humans are hardly able to identify three or more odor components in a mixture that contains up to eight odorants.[24] This perspective can be seen as analogous to physical objects recognized with visual perception. When you see e.g. a cup of coffee, you recognize it as such without individually inspecting every little detail of the object. Similarly, when you smell the coffee in that cup, you don't individually analyze every odor component found in the complex mixture but identify the odor object as coffee.[22], [25]

2.2 Artificial olfactory system

Detecting and classifying odors has been implemented in many applications. Using human nose as the detector is an obvious choice but it also has drawbacks like subjectivity, infections, exposure to hazardous materials and often it is not economically reasonable to invest in training for tasks taking only a short time.[2], [22] Still, even the best artificial odor detectors are not at the level of vertebrate nose although big advances in the field of sensors and instrumental odor detection systems have been made in recent times, e.g. Tang et al. presented an electronic nose system capable of classifying three different fruits[26] and Omatu et al. presented the odor classification of different species of coffee and tea.[27] The current superiority of vertebrate nose is the reason why dogs and other

animals are still widely used as olfactory detectors with notably better detection sensitivity and specificity when compared to human nose.[28] This difference in operation is due to a few key factors. Dogs have larger area of the epithelium and surface area of the cilia compared to humans.[1] Another key factor is the functioning and structure of the canine nose, which has muscles actively sniffing with a frequency of approximately 5 Hz.[29] These coupled with the unique nasal airflow patterns of canine nose is the reason why the olfaction of dogs is so sensitive and effective.[30], [31]

Olfactometers and other instruments for artificial olfaction can be divided into three main parts: a sample handling system, a detection system and a data processing system. This makes considering such a complex system more approachable.[15]

2.2.1 Sample handling system

When considering an artificial olfactory system, being able to provide a reliable and consistent odor sample is a crucial part in any e-nose instrumentation. Although a lot of attention is usually given to the selection of the sample analyzer, same amount of attention is not often given when considering the sample handling system.[15] Errors and inconsistencies in sample delivery will induce more errors in detection and odor classification. This is especially important when using sample delivery system to test, calibrate and validate new sensors or systems.[13]

First thing to consider in designing a sample handling system is the phase of the desired sample that is being provided for the detection system, liquid or gas. The source for the odor is the next thing to be considered, it can be in liquid or gas but also solids are used. If the sample is delivered to the detection system in liquid and if the odor component being provided is already in a solution with known concentration, the system can be constructed relatively easily using pumps and tubing. However, as providing the sample in liquid is not analogous to the natural olfactory system, often using gas phase samples is desired. When the sample is provided in gas phase the system also grows in complexity as there must be some form of evaporation unit if the odor component is not naturally in gas phase, which often is the case.

Using permeation tubes is a popular technique to emit certain compounds at a constant rate when they are under constant temperature. Permeation tube is a small permeable tube filled with a pure chemical compound with the objective to achieve an equilibrium state between gas and liquid (or solid) phase. The typical permeation rate is in the magnitude of milligrams per day. [32], [33]

Various methods have been developed and presented in the field of evaporation that are used in e-nose instrumentation. In evaporation, a molecule is transported across liquid-gas –interface. Evaporation occurs at the surface of a liquid when molecules with the highest kinetic energies escape into the gas phase. Even though its great importance in

many fields of technology and science, the fundamental understanding of the phenomenon is still lacking.[34] However, four key parameters for evaporation have been identified; the surface area of the liquid free to evaporate, the temperatures of the carrier gas and liquid, the relative humidity of the gas and the movement of the gas. Evaporation can be increased with these parameters by increasing the surface area, increasing temperatures and using as dry as possible carrier gas that is moving across or through the liquid in a fast velocity.[35]

Static headspace (SHS) is a relatively simple technique, where the sample is placed in closed container and is let to evaporate. When equilibrium is reached in the container, the gas phase sample is extracted. Extraction is done either manually with gas-tight syringes, or by balanced-pressure or pressure-loop –systems. After extraction, sample is injected in the analyzing system (Fig. 4). [15], [16]

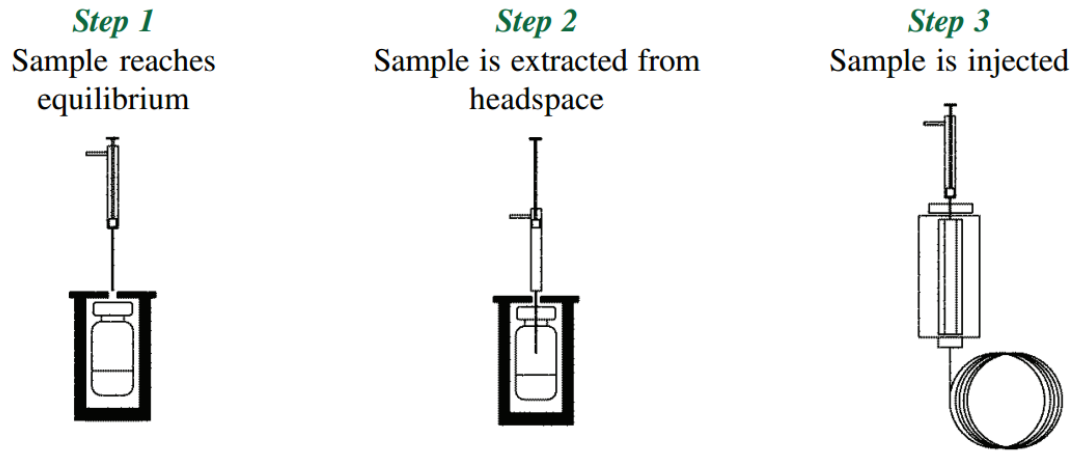

Figure 4. The protocol of static headspace sampling. After sample reaches equilibrium in the container, it is extracted and injected in the analyzing system. [16]

Purge and trap (P&T) and dynamic headspace (DHS) techniques are used in wide range of environmental and industrial applications, often to extract samples to be analyzed further e.g. with GC-MS. [36]–[38]

The drawback using sampling methods introduced above, is that it is not possible to produce continuous, long lasting gas flow with a stable concentration. One of the more novel approaches was presented by Hashimoto et. al[39]. They presented a tiny olfactory display using surface acoustic wave device and micropumps to produce odors to be potentially used in wearable devices. In this work, another novel approach to sample handling, addressed in more detail in chapter three, is presented using programmable syringe pumps and ceramic heating elements in order to produce continuous odor gas flows with stable concentrations.

2.2.2 Detection system

The principle of the sensor array in artificial olfaction is very similar to olfactory receptor cells and nerves in the human olfactory system. The array is the heart of e-nose –systems and is responsible for feeding the measured data from sensors to data processing unit. The range of different sensor technologies is vast and growing, but some common principles can be applied when considering their performance. A good sensor for e-nose should fulfill a number of criteria. Most importantly, the sensor should have high sensitivity to the intended group of chemical compounds it is designed to detect with a threshold of detection similar or lower to that of a human nose.[12] The desired selectivity depends on the implementation; for a sensor array with high number of sensors high selectivity can be beneficial if each sensor is able to detect different VOCs. As e-noses are often used in uncontrolled environments, the stability of the sensor against changing temperature and humidity is also important, but often hard to achieve.

The effect of gas atmosphere composition on the conductivity of semiconducting metal oxides has been known and studied for more than half a century. First experiments were made observing the interactions of conductivity of ZnO and the gas atmosphere. Based on the results, further metal oxides were considered and examined in regards to their conductivity to varying gas atmosphere. Metal oxides such as TiO_2 and SnO_2 were proven to have a good property in varying their conductance over different gas compositions. Gas sensors based on semiconducting metal oxides have stayed relevant all these decades and they are the most widely used group of gas sensors. The interest in metal-oxide sensors has remained due to their many useful properties; the possibility to detect large number of different gases, relatively simple working principle, low cost and flexible manufacturing.[40]–[42]

At first, the development of gas sensors using metal-oxides aimed primarily in developing sensors able to warn of explosive gases. The primary market for these was in Japan due to legislation requiring the use of such detectors in households. The legislation was put in place as detecting combustible and dangerous gases is of particular interest in the densely built Japanese cities where gas furnaces and wooden houses were common as well as the rapidly developed industry where the usage of various gases increased. The worldwide market for gas sensors in 2012 was estimated to be 2.5 billion euro, of which the Japanese market alone still covers 20%.[43]

The first-generation metal-oxide gas sensors, where the initial essential properties (affordable price for a regular household, sufficient sensitivity to relevant gases and an adequately long life span) were implemented also exhibited many unpleasant features limiting their use. These off-putting characteristics included high cross-sensitivity to gases not to be measured, high sensitivity to changing humidity and temperature, long-term drifting of signals and long, up to 50 hours, break-in time.[42]

Metal-oxide sensors have come a long way since the first-generation applications and many off-putting characteristics can be minimized as the research and development in the field of material technology has been rapid in the 21st century. One of the latest products relying on metal-oxide sensors is a Multi-Pixel Gas Sensor SGP30 (Sensirion, Switzerland). SGP30 is a MEMS metal-oxide gas sensor for measuring VOCs and although not yet released for the market, available preliminary data sheet[44] claims it to have outstanding long-term stability, a very small package, low power consumption and claims to be "the first metal-oxide gas sensor featuring multiple sensing elements on one chip".[44]

The advancements in material technology have also enabled the development of other types of sensors with various different operating principles. Conducting polymer (CP) sensors have high application potential for chemical and biological sensors. The conductivity of CP in an uncharged state is almost nonexistent. Intrinsic conductivity for these materials is achieved by doping them either by oxidizing (p-doping) or reducing (n-doping), which forms charge carriers that are responsible for the conductivity. [45] Single CP sensors typically have poor selectivity, which often leads to using different chemical CP sensors in an array, which are used for both for gaseous and liquid analytes. CP sensor arrays have been used in various fields, e.g. defining aromas or taste of food products, detecting pollutants in water, monitoring emissions from sewage plants and monitoring possible infections in wounds[46].

Although generally more complicated than other sensors, optical sensors have also been widely used as chemical sensors. Big advantage with optical sensors is that their response can be well defined and precisely measured. They also provide various measuring possibilities; when light source of the sensor excites volatile molecules, the signal can be measured as an absorbance, reflectance, fluorescence, refractive index, colorimetric or chemi -luminescence.[15] Advances in producing nanoscale structures have also opened new possibilities regarding to sensor manufacturing. Structures such as nanowires, nanotubes and nanofibers have attracted a lot of attention in physical, chemical and biological sensing. [47] These nanostructures have unique geometry with low dimensions and large surface-to-volume ratio, properties which are valuable in sensing elements. An artificially intelligent nanoarray consisting of a random network of single-walled carbon nanotubes and molecularly modified gold nanoparticles was presented by Nakhleh et. al.[48] The nanoarray was used to study human breath samples from 1404 subjects having one of 17 different disease conditions. Each disease was shown to have its own unique "breathprint" and the nanoarray was able to achieve an accuracy of 86% to detect and discriminate between different disease conditions.[48]

Progress in material engineering and the better understanding of real olfactory systems in living creatures has also enabled the production of biomimetic sensors. These sensors aim to mimic the natural olfaction by using the same exact components that can be found in a natural olfactory system; ORs, odorant binding proteins (OBPs) and OSNs. These components can be harvested from living creatures, such as insects. Whole insects have been

demonstrated to work as sensors themselves[49]. Another way to develop olfactory receptor –based sensors is to synthesize artificial peptide sequences to mimic the binding site of OR or OBP.[41], [50]

In this work, instead of the usual solutions, the detection system in the constructed olfactometer is an aspiration ion mobility spectrometer (aIMS) device. The use of aIMS is a quite novel approach in the field of olfactometry. Theory of IMS is considered in detail in section 2.3.

2.2.3 Data processing system

The information gathered by the detection system can be sent to a display for human analysis. The information from the sensor array can also be sent to computer emulating a human nose to perform automated analyses that rely on methods like statistical pattern recognition, neural networks and chemometrics. All these pattern recognition methods consist of several stages of data processing. First the multivariate sensor data is pre-processed, where the data curves are often smoothed, drift compensated and outliers eliminated. Secondly, the extraction of the features from the pre-processed data for the pattern recognition method used is carried out. Feature extraction from the sensor array inputs is a crucial step to ensure that the extracted features contain useful and relevant information from the sensors. Thirdly, a classifier is used to determine to which predetermined class the given detection system outputs correspond. Finally, the accuracy of the model can be estimated with additional data. [15] The analysis and interpretation of the data can be carried out using a variety of different approaches. Commercially available analysis techniques used in electronic noses consist of three broad categories: multivariate data analyses (MDA), network analyses and graphical analyses.[12]

MDA consists of a wide set of different algorithms, many of which have also been utilized in artificial olfaction systems as MDA is very useful with sensors having partial-coverage sensitivities to individual compounds in a complex mixture.[12] Principal component analysis (PCA) was presented in 1901 by Karl Pearson and it is a common statistical method for finding patterns from high-dimensional data. In general, PCA can be used to simplify almost any data matrix. It is often used in applications such as face recognition and image compression. PCA uses orthogonal transformation to convert a set of data containing possibly correlated variables into a set of linearly uncorrelated variables, called principal components.[51]

Artificial neural networks (ANNs) try to mimic the cognitive processes of a human brain, being in other words mathematical representations of the human neural architecture.[52] The computations in a human brain are done by interconnected neurons interacting with each other. Similarly, ANN has interconnected data processing algorithms working in parallel. To make ANN-module able to classify unknown datasets, it must first be taught using some form of training database. Various methods for instrument-training have been

employed and the training process requires certain amount of reference data samples with known classifications. ANN is the most evolved analysis technique used in commercial e-noses.[52], [53]

In 1969, John W. Sammon introduced a new nonlinear mapping algorithm for multidimensional scaling[54], which means that it represents high-dimensional information in a space of lower dimensionality. This mapping method was named after the inventor and the main property of Sammon mapping is that it retains the geometrical distances between signals when scaling down from multidimensional space to two or three-dimensional space. Using Sammon mapping is a useful method for determining the shape and density of data clusters and visualizing the relative differences between clusters. [55], [56] Some of the data produced with the presented olfactometer is presented and analyzed using Sammon mapping in chapter four.

2.3 Ion mobility spectrometry

IMS refers to "principles, methods, and instrumentation for characterizing substances from the speed of swarms (defined as the ensembles of gaseous ions) derived from a substance, in an electric field and through a supporting gas atmosphere" [57]. This broad definition includes the different developed variations of IMS with different geometry, working conditions (pressure, flow, composition of gases) and the strength and control of electric fields. These include the most traditional drift tube ion mobility spectrometry (DTIMS), aIMS and field asymmetric ion mobility spectrometry (FAIMS) together with differential mobility spectrometry (DMS), both of the last two also referred collectively as differential ion mobility spectrometry (DIMS).[57]

DTIMS consists of the ionization chamber, also called reaction region, containing the ion source and ion shutter, the drift region and the Faraday-plate detector (Fig. 5). An electric field (E in V/cm) is applied along the device to enable the drifting of ions. A continuous stream of carrier gas containing the analyte is ingested in the reaction region and passes the ionization source. The source most used and understood for IMS is radioactive ^{63}Ni source [57]. In general, radioactive sources provide many advantages such as no need for external power supply and no moving parts. Still, the use of radioactive sources is discouraged mainly because of regulatory reasons as radioactive sources require special permits and licensing procedures. There are also various other ionization techniques used in IMS, e.g. corona discharges, photoionization and electrospray.[57] Currently the development of pulsed corona discharges seems to be the most promising alternative for radioactive sources as it consumes little power, lasts long time and operates in both positive and negative mode.[58]

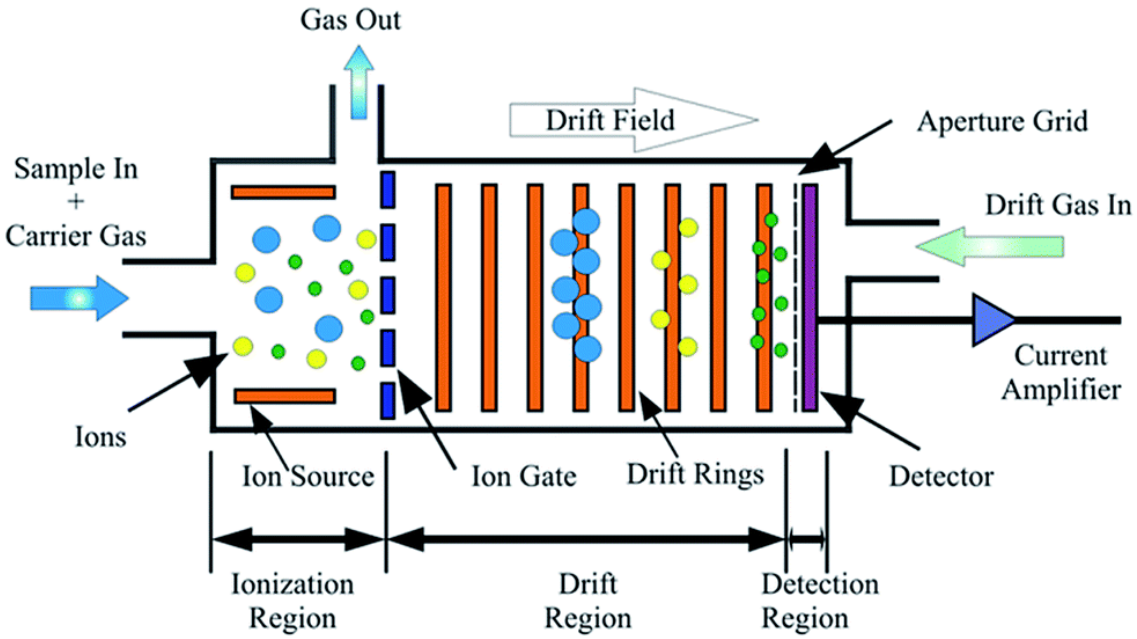

Figure 5. The structure of conventional DTIMS instrument. The sample being examined is directed to ionisation region, from where the formed ions are released in pulses by the ion gate to the drift region. There, according to the mobility of different ionic species, ions drift to the detector plate due to the electric drift field.[71]

The ion shutter, also called a shutter grid or ion gate, is a metal wire grid that spans over the whole cross section of the drift tube. The ion gate is "closed" when large voltage differences between adjacent wires are applied. In this situation, the drifting ions near the gate are drawn to wire surfaces, neutralized and the neutral products are ejected from the system with gas flow. In predetermined cycle, the electric field in the shutter grid is eliminated or made weak enough to open the gate and let the ions flow past the gate to the drift region. The major disadvantage of the traditional DTIMS devices is the lack of real time signal gathering due to the shutter grid releasing the ions in pulses, the interval between pulses being normally 10-30 milliseconds.[57]

In the drift region, the swarm of ions travels along an electric field gradient which separates the swarm in groups based on the mobility of the ions. Faraday plate as the detector neutralizes the ions that drift to its surface. As the charge of the ions neutralize, the detector produces an electric signal and the intensity of this signal is related to the charge of a single ion and the size of the group. The time point when the signal is detected is related to the mobility of the group. This means that the drift time, t_d, of ions is directly related to the mobility of the ions and that is why the technique is also called time-of-flight (TOF). The drift velocity of an ion, v_d, can be represented by

$$\boldsymbol{v_d = \frac{d}{t_d}} \qquad (1)$$

where d is the distance travelled, typically from 4 to 20 cm in modern IMS analyzers. Normalizing the drift velocity to the electric field E produces the mobility coefficient K:

$$\boldsymbol{K = \frac{v_d}{E}} \qquad (2)$$

The temperature (T) and pressure (P) inside the drift tube affect the drift velocity and the value for K is commonly normalized to 273 K and 760 torr. The changing conditions can be taken into account by calculating the reduced mobile coefficient K_0:

$$\boldsymbol{K_0 = K \cdot \frac{273}{T} \cdot \frac{P}{760}} \qquad (3)$$

K_0 is commonly used to describe ion mobility but using it is also problematic as the mobility formulas are derived from studies conducted in nonclustering atmospheres, in pressures often as low as 1 to 10 torr. Calculated values for K_0 correspond well to reality in such low pressures and with nonclustering gases such as He. However, problems arise particularly in ambient pressure and with polarizable gases, where the pressure and temperature alone cannot accurately describe the changes in ion mobility. When operating in these kind of conditions, also gas temperature, pressure and gas composition should be taken in to account for getting a more accurate value for ion mobility.[57]

Another factor affecting the reduced mobility K_0 is the ratio between electric field and the number density of the carrier gas. This ratio is presented as

$$\boldsymbol{Td = \frac{E}{N} \cdot 10^{17} V\ cm^2} \qquad (4)$$

where when E is given in volts and N in particles per cubic centimeter, the ratio is given in the units of towsends (Td) as one townsend equals to $1 \cdot 10^{-17} V\ cm^2$. The relationship between Td and K_0 is similar for all ions and buffer gases, and three distinct regions can be found. In a low-field region the reduced mobility is constant as a function of Td, in an intermediate-field region the reduced mobility increases when increasing Td and in high-field region the reduced mobility decreases when increasing Td.[57] Different regions are used with different IMS technologies and devices; the region where the mobility is constant is the region where DTIMS, aIMS and differential mobility analysis (DMA) are normally operated and the regions where the mobility changes as a function of Td are the regions where DMS and FAIMS normally operate.[57], [59]

2.3.1 Ionization physics

Ions are formed in ion mobility spectrometers when neutral molecules in the analyte undergo a series of ion-molecule reactions with reactant ions. The process from neutral analyte to product ion is different for positive and negative ions as the reactant ions are also respectively positive or negative. When air is used as the carrier gas, the dominant reactant ions are hydronium ions $H^+(H_2O)_n$ to produce positive ions and hydrated oxygen $O_2^-(H_2O)_n$ for negative product ions, where n is dependent of the moisture content of the gas and its pressure and temperature.[57]

In formation of positive ions, the analyte molecules M form cluster ions when colliding with hydrated protons:

$$\boldsymbol{M + H^+(H_2O)_n \leftrightarrow MH^+(H_2O)_n^* \leftrightarrow MH^+(H_2O)_{n-x} + xH_2O} \quad (5)$$

This reaction determines the transformation efficiency of molecules into ionic products. This compound-dependent parameter proton affinity (PA) defines the probability of the reaction. PA is related to the energetic effect of proton transfer reaction and it is defined as the relationship of enthalpies in formation of MH^+ and its neutral counter M.

Experiments studying chemical ionization under atmospheric pressure have indicated that compounds can be divided in two distinct groups based on their behavior in Equation 5, substances with high and low PA. For substances with high PA the reaction (5) moves almost solely forward. Typical members in this group are ammonia, amines and organo-phosphorous compounds. With these compounds, the quantity of the reaction product is depending on the kinetics of the system. This means that every analyte molecule, that has possibility for effective interaction with reactant ions, will be transferred into ionic form. The group with compounds having high PA is also called “kinetic group” as the quantity of product ions are kinetically controlled. [60]

The second group, compounds with low PA, consists of ketones, alcohols and many other organic compounds. For these, the reversal of the reaction of proton attachment in reaction (5) is significant. Therefore, here the quantity of reaction products is defined by the reaction equilibrium. Because chemical equilibrium is dependent on the systems thermodynamics, this group is also called “thermodynamic group”.[57], [60]

If the vapor concentration of M is high enough, a second product ion can form as another neutral analyte molecule attaches to the previously produced protonated monomer to form a proton bound dimer:

$$\boldsymbol{MH^+(H_2O)_n + M \leftrightarrow M_2H^+(H_2O)_{n-x} + xH_2O} \quad (6)$$

The attachment of additional analyte molecules is also possible, but the lifetimes of such trimers and tetramers in the purified atmosphere of the drift region is so short that they rarely affect the observed mobility spectra.[57], [60]

For negative ions, on top of the dominant reactant ions also various other ions are formed. For air as the carrier gas, the formation of very diverse set of reactant ions such as Cl^-, $(H_2O)OH^-$ or NO_2^- is possible, but the concentration and the influence on ionization of these is usually negligible. Association of a molecule and an oxygen anion forms the product ions in negative polarity:

$$\boldsymbol{M + O_2^-(H_2O)_n \leftrightarrow MO_2^-(H_2O)_n \leftrightarrow MO_2^-(H_2O)_{n-x} + xH_2O} \quad (7)$$

Electron affinity (EA) is the compound-dependent parameter to be considered in formation of negative ions. Simply put, EA is the likelihood of neutral atom gaining an electron. It is defined as the change in energy (kJ/mole) of a neutral atom in gas phase when an electron is added to the atom. Electron capture is possible for any analyte with positive EA.[61]

When using a radioactive source for ionization, it is noted that ionization of substances with low PA is reduced when compounds of with high PA are present. Same applies in the formation of negative ions; ionization of substances with lover EA is hindered if substances with high EA are present.[62]

2.3.2 Aspiration ion mobility spectrometry

The structure of aIMS instrument is different in comparison with DTIMS and the most notable differences are that the electric field gradient and the carrier gas flow in aIMS are perpendicular to each other and that there are multiple detector plates placed on the sides of the drift region. The structure of aIMS instrument is seen in Figure 6.

Ions entering the drift region in aIMS start to deflect to the sides of the region due to the direction of the electric field. The ions with high mobility deflect faster than the low mobility ions and are observed on plates closer to the ionization chamber. Ions with lower mobility drift longer before they are deflected to the chamber walls and are detected on the further electrodes. No need for the shutter grid makes the structure of the device simpler and enables signal recording with 100 % efficiency as gas flows continuously to the drift region.[57], [63]

When compared with DTIMS and DMS, aIMS has less to offer in terms of resolution and selectivity. Nonetheless, aIMS provides many advantages being very robust and easy to use. The aIMS instruments are handheld devices with fast response times and low energy consumption. The relatively low cost (< 10 000$) is also an advantage compared with commercial DTIMS and DMS devices, which usually have a price tag between 10 000 – 100 000 $.[64]

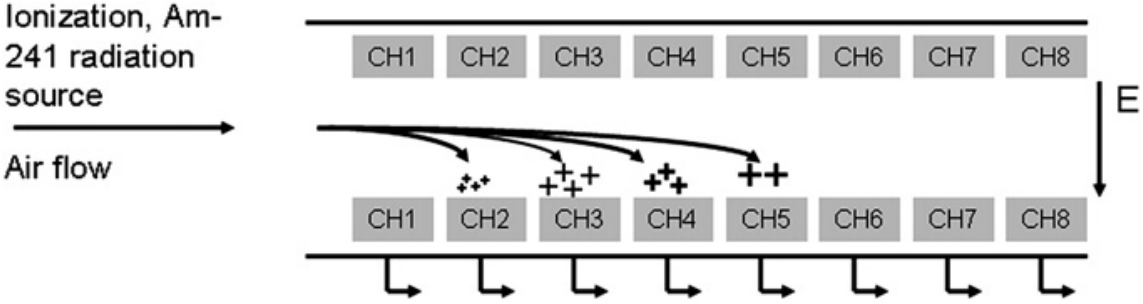

Figure 6. Structure of aIMS. The carrier gas containing the molecules of interest is directed to the ionization chamber, from where the formed ions flow in the drift region and start to deflect to the sides due to the perpendicular electric field according to the mobilities of different ionic species.[63]

Applications with aIMS are in large part limited to detecting CWAs and TICs and are not that widely involved in scientific research. Still, especially due to the mobility of the devices, applications like detecting human metabolites from entrapped volunteers have been studied.[64], [65] As mentioned, and explained in more detail later, in this work an aIMS device is used to monitor the output gas flow of the introduced olfactometer instrument.

2.3.3 Differential ion mobility spectrometry

Differential ion mobility spectrometry adds an additional layer of complexity in comparison with aIMS but that layer also provides better separation. The basic structure between DMS and aIMS is similar, but the key differences are that in DMS the applied electric field strength is higher and the field is not constant, but is oscillated between a high positive and a low negative voltage. This enables the better separation as the ion mobility has a specific dependence on the field strength that is not apparent in low fields. At higher fields, the ion mobility for different ionic species can change in either direction or can change in different directions in different field strengths.[66], [67]

The alternating voltage is applied and designed so that the product of voltage and the pulse duration is identical for the positive and negative voltage (Fig. 7). If the mobility of an ion is the same under high and low fields, the ion moves upwards during the high voltage cycle the same amount as it moves downwards during the low voltage cycle producing a net movement of zero. The peak voltage of the waveform is called dispersion

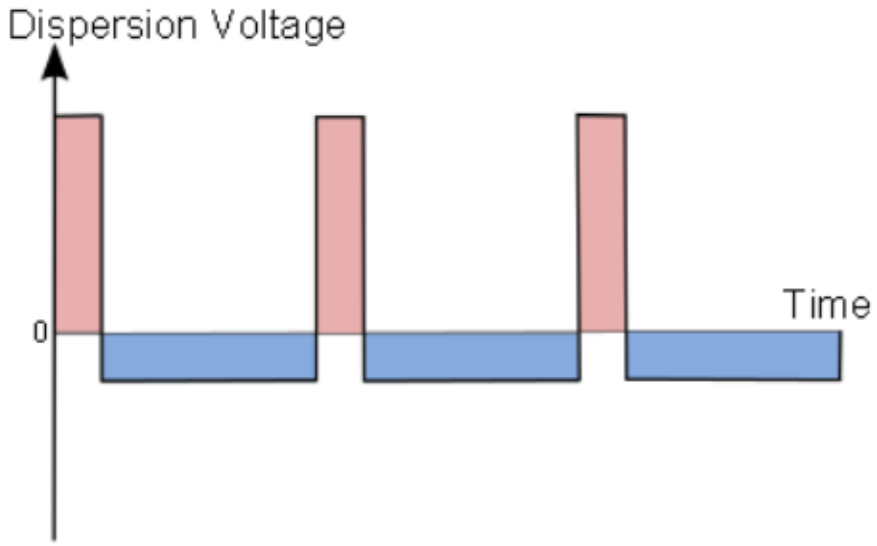

Figure 7. The alternating square wave applied in DMS separation. The product of the voltage and the pulse duration are identical for the positive and negative segment of the waveform.[67]

voltage (DV). As the mobility of different ionic species differs in the high field, the net movement of an ion can also be either positive or negative (Fig. 8).

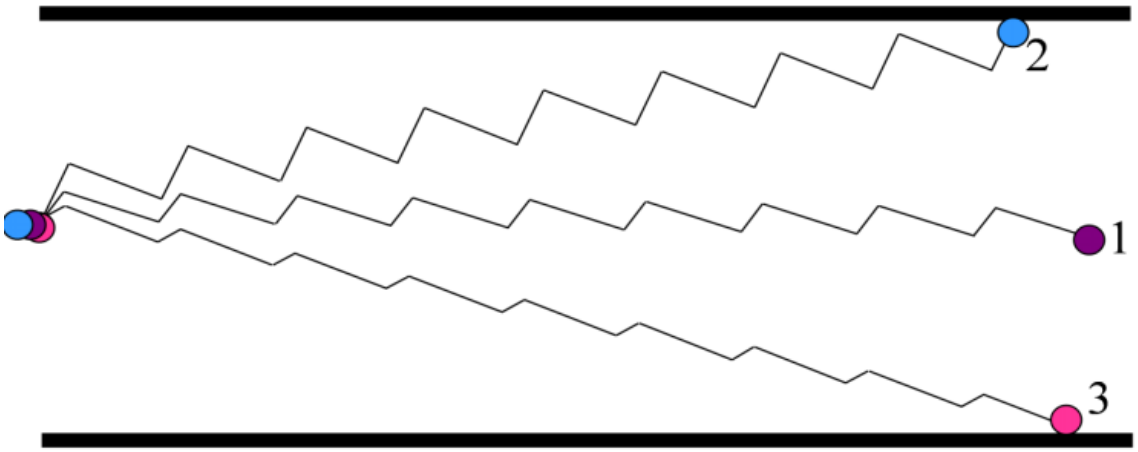

Figure 8. The movement of different ion species under the alternating voltage. Ion 1 experiences a net movement of zero, while ions 2 and 3 experience positive and negative movements.[67]

The drift of an ion towards one of the detector plates can be stopped by applying an additional voltage, compensation voltage (CV). If CV is applied with appropriate polarity and magnitude, the drift of the ion towards the plate is stopped, or "balanced", and the ion will flow through the drift region of DMS without touching the plates. Correct settings for CV are compound-dependent, e.g. for chloride with high ion mobility in high fields the necessary voltage to stop the ion is also high. Each type of ion has a characteristic value of CV and by applying CV with different parameters, the ions with balanced drift is changed. So the DMS can be seen as ion filter capable of selective transmission of only wanted ionic species.[59], [68]

2.3.4 Ion mobility spectrum

Three different approaches for the separation of ions by gas phase mobility have been presented: temporal, spatial and focusing. Temporal separation works by recording the arrival times for the pulses of ions traveling axially through the drift region and it is achieved using DTIMSs and traveling wave ion mobility spectrometers (TW-IMSs). When a swarm of ions arrives at the detector electrode, the peak in current produced by the ions represents the arrival time of the swarm. Ion mobility K in the case of temporal separation is determined from equation (3).[57] An example readout from DTIMS is presented in Figure 9.

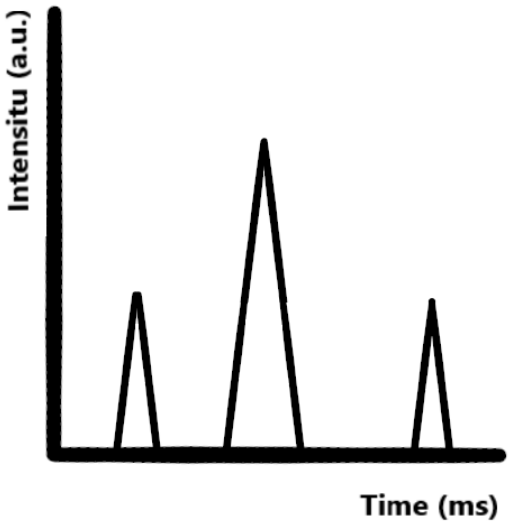

Figure 9. A basic form of DTIMS response. Each peak corresponds to a group of ions with the same mobility arriving to the detector plate. The intensity of the peak is determined by the total charge of each group of ions.

Mobility spectrum produced with spatial separation, associated with aIMS, can be represented as a histogram of response, one from each electrode. This kind of readout can be interpreted as a fingerprint for the odor or mixture of odor components being detected (Fig. 10). The readings from the aIMS electrodes can also be read over longer period of time, plotting a figure with channel responses as function of time (Fig. 11).

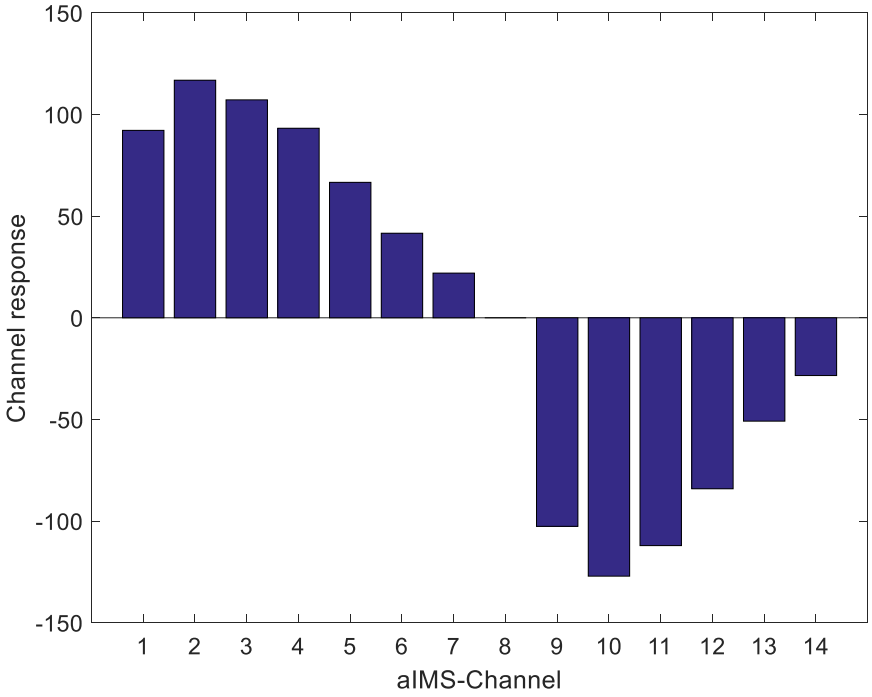

Figure 10. An example readout for aIMS-device. Each bar corresponds to a signal from a single electrode at a single point in time.

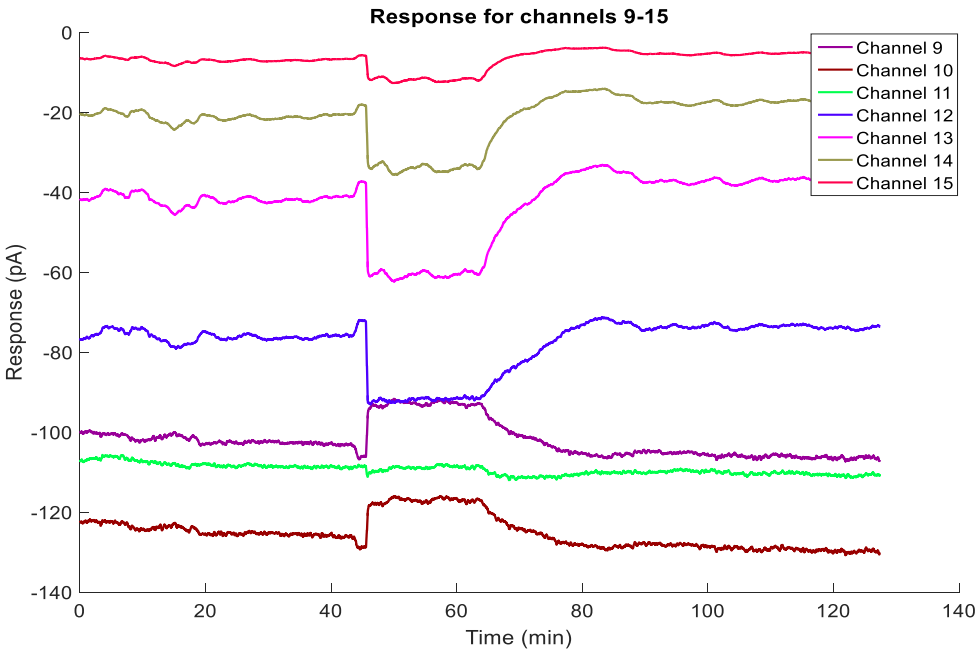

Figure 11. A plot for channel responses for the negative channels of aIMS instrument ChemPro 100i.

In focusing separation, achieved with the oscillating electric field in DMS, the ion current detected on the detector is plotted as a function of the compensation voltage for different values of DV (Fig. 12).

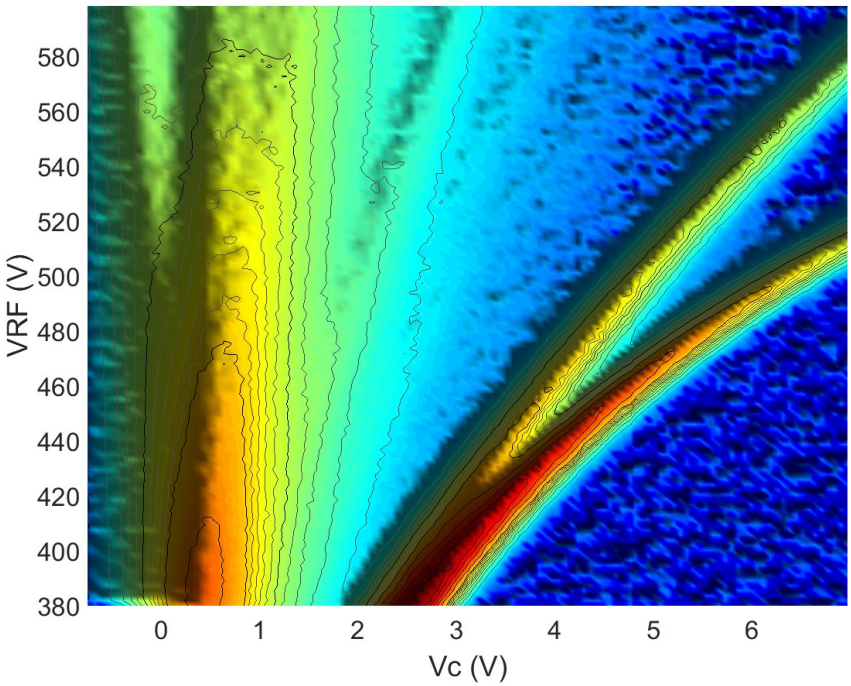

Figure 12. An example spectrum of DMS device. The spectrum is essentially an intensity map showing the amount of ions passing to the detector for different values for DV (VRF) and CV (Vc).

3. MATERIALS AND METHODS

A novel approach for a compact olfactometer containing a developed sample handling system coupled with ChemPro 100i (Environics, Mikkeli, Finland) aIMS-device is presented. The system is able to produce three different gaseous odor components and vary their produced gas concentrations.

3.1 The chosen odor components

Measurements were conducted using the three main components identified in jasmine oil: benzyl acetate (BEA), cis-jasmone (CIS) and indole (IND). As IND is in powder form in standard room conditions, these components were diluted using propylene glycol (PG) as our sample handling system can only handle samples in liquid form. Even though propylene glycol is a viscous, colorless and odorless liquid, using a diluent is not an ideal solution as it also most likely produces signal in the detection unit and the data processing and analysis becomes more complex. Using diluted solutions was beneficial in terms of making the different components similar in properties, mainly the vapor pressure, which can be calculated from Raoult's law. The law states that "the partial vapor pressure of each component of an ideal mixture of liquids is equal to the vapor pressure of the pure component multiplied by its mole fraction in the mixture".[69] Similar properties when using solutions with the low concentration of the odor component (< 20 % w/w) made it possible to use the same power control settings, described in more detail in 3.3, for each of the three components.[70]

3.2 Environics ChemPro 100i

ChemPro 100i (Figure 13) is a handheld chemical detector initially designed for field detection and classification of CWAs and TICs. ChemPro 100i is based on aIMS technology and it contains 14 ion-detecting sensor plates, seven for positive and seven for negative channels. The device has ^{63}Ni as the ionization source. On top of these sensors, ChemPro 100i also contains additional metal-oxide sensors, which were not included in

Figure 13. ChemPro 100i

the older model. These sensors were added to circumvent problem of identifying exhaust fumes from vehicles as CWAs as the device is intended for mobile use in the field.

The ChemPro 100i was used in this work in measuring the output airflow of the introduced olfactometer. The device had a crucial part when first designing the system in verifying the stable production of the odorants in gas phase. Even though the ChemPro 100i is developed for mobile use, it can also be used connected to a computer and signals can be inspected in real time with software provided by Environics. The log-file that the ChemPro-software produces is a matrix with 59 colums. Values for each column are recorded in one second intervals. On top of the readings from 14 channels, the log-file also contains a lot of other information and metadata, such as the date and time, external and cell temperature as well as relative and absolute humidity.

3.3 The implemented sample handling system

The introduced compact olfactometer and sample handling system (Fig. 14) was initially designed for the three odor components mentioned in 3.1. The main objective of the sample handling system, and thus the whole olfactometer, was to provide different odor components in different concentrations in gas phase with relatively low-cost components. The mixture of the different components was also wanted to be varied. This lead to a design where each of the components were evaporated in individual evaporation units (Fig. 15). The frame structure for the evaporation units is a 3D-printed object designed using

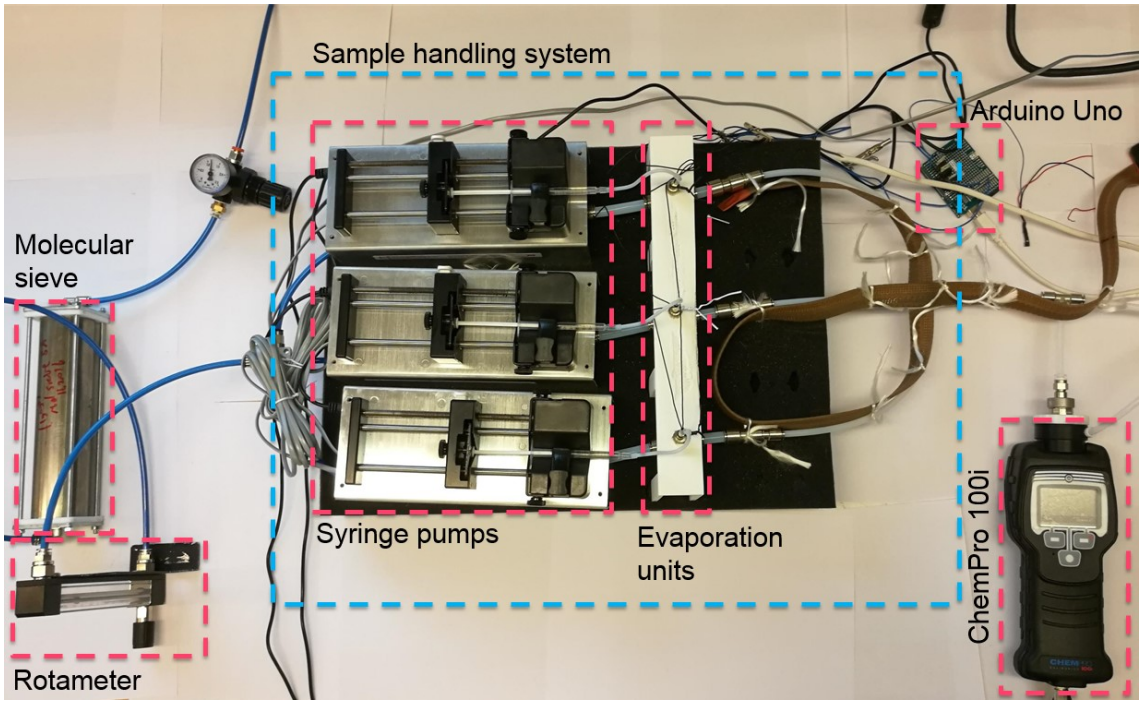

Figure 14. The constructed compact olfactometer in our laboratory setup with sample handling system and the main components of the system identified.

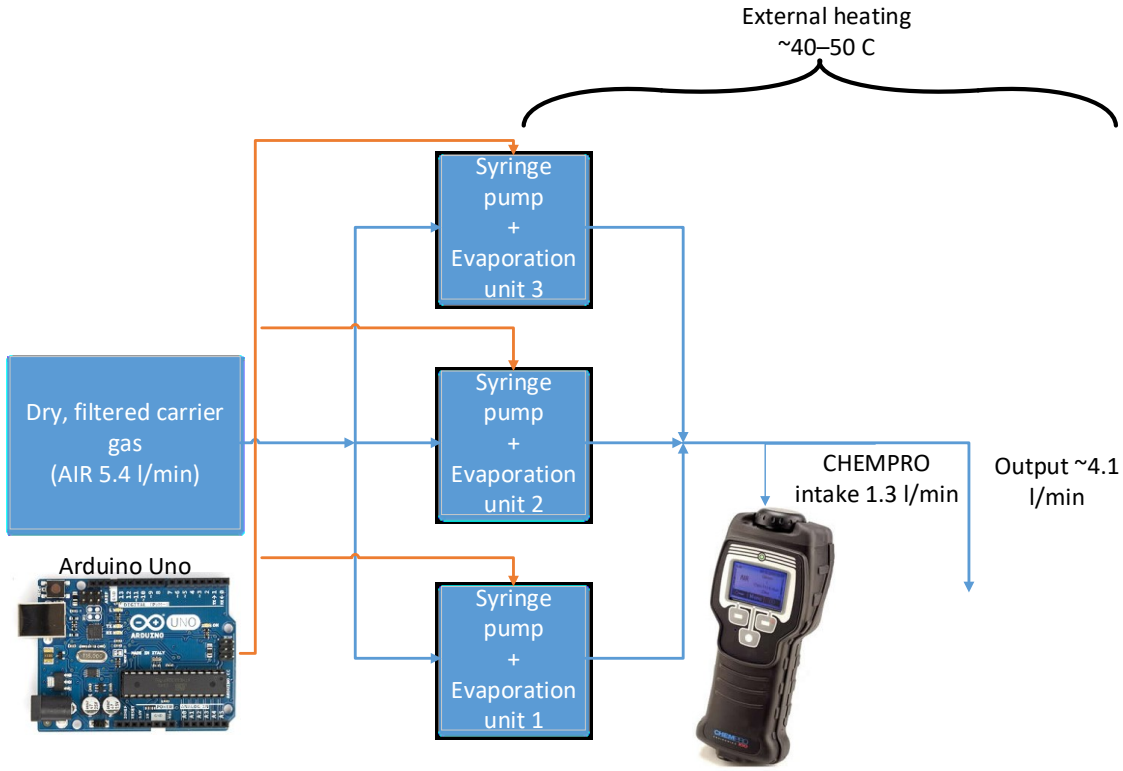

Figure 15. Block diagram of the introduced compact olfactometer. Dry and filtered air is directed evenly to three channels, each having their own evaporation unit. Output gas flow of the system is connected to ChemPro 100i. The remaining gas flow of 4.1 l/min can be directed to waste filter or in human perception testing to participants nose.

SOLIDWORKS® 3D computer-aided design software (SolidWorks Corporation, USA). Air was used as the carrier gas and it was dried and purified with 5Å molecular sieves

(Alfa Aesar, Germany) and activated carbon. The total carrier gas flow of the system is controlled by Q-flow rotameter (Vögtlin Instruments, Switzerland) and each channel has a flow of 1.8 l/min. Due to the geometry of the systems pneumatic tubing, initially the flows of channels one and three were identical but different to channel two. A flow limiter was installed in the channel two and with right settings identical flow was achieved in all the three channels. The flows were verified using Gilibrator-2 calibrator (Sensidyne, USA). Junk odor flows were pushed through activated carbon cylinder.[70]

Each evaporation unit consists of basic pneumatic components, a ceramic heating element and polyether ether ketone (PEEK) tube that connects the syringe tubing on the surface of the heating element (Fig. 16). PEEK is a material with good heat resistance having a high glass transition temperature of 143 °C, which makes the placement of the tube on the heater surface possible but is then also the maximum possible temperature that the heating elements are allowed to have. For the heating elements used, surface temperature of 140 °C corresponds approximately to 1.5 W of power.[70]

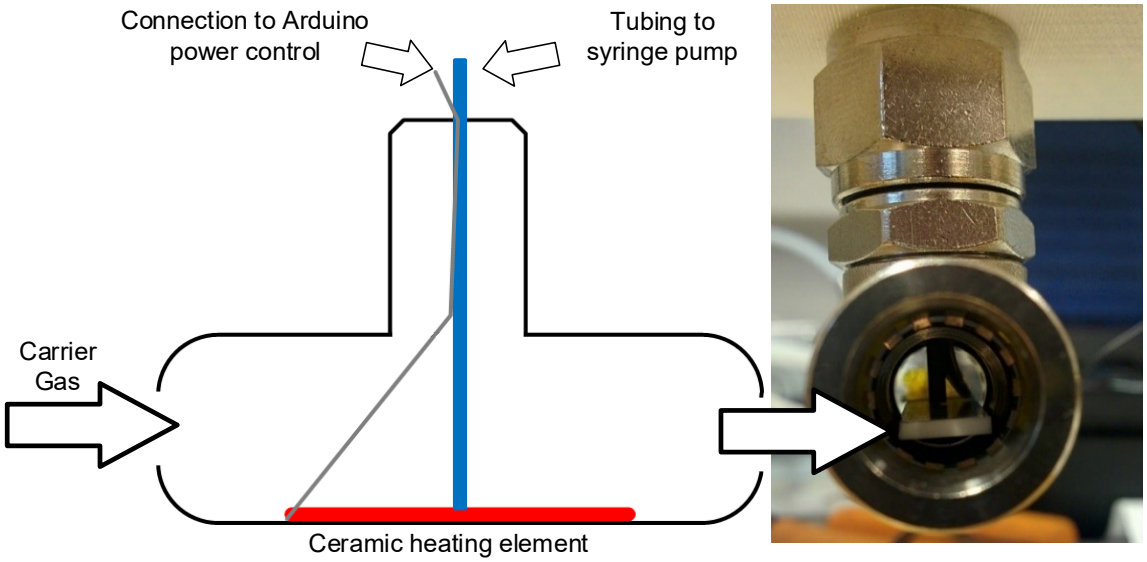

Figure 16. Structure of the evaporation unit. The diluted odor component is directed to the surface of ceramic heating element through heat resistant PEEK-tube.[70]

The diluted odor component is pumped through the tube using a syringe pump, one for each odor component. We used Newera NE-500 (New Era Pump Systems Inc., USA) programmable syringe pumps and they were controlled with Matlab (The MathWorks, USA) taking advantage of the existing function library written for the pumps. The pumps are controlled by programming different phases to the pumps. Each phase is responsible for certain task, e.g. pumping with set speed and time, stopping or waiting certain time before moving to next phase. For our system, the most important function of the pumps is the ability to produce stable, constant pumping with a known flow rate.[70]

The electric powers of the ceramic heating elements are controlled with metal–oxide–semiconductor field-effect transistor (MOSFET) power circuit built on Arduino Proto Shield Rev3 (Arduino) (Fig. 17). According to the gate voltage of each MOSFET, the voltage and current over and through the heating element changes. The heating powers are calculated from the tabulated values of the current and voltage for different gate voltage values using equation

$$\boldsymbol{P = UI} \qquad (8)$$

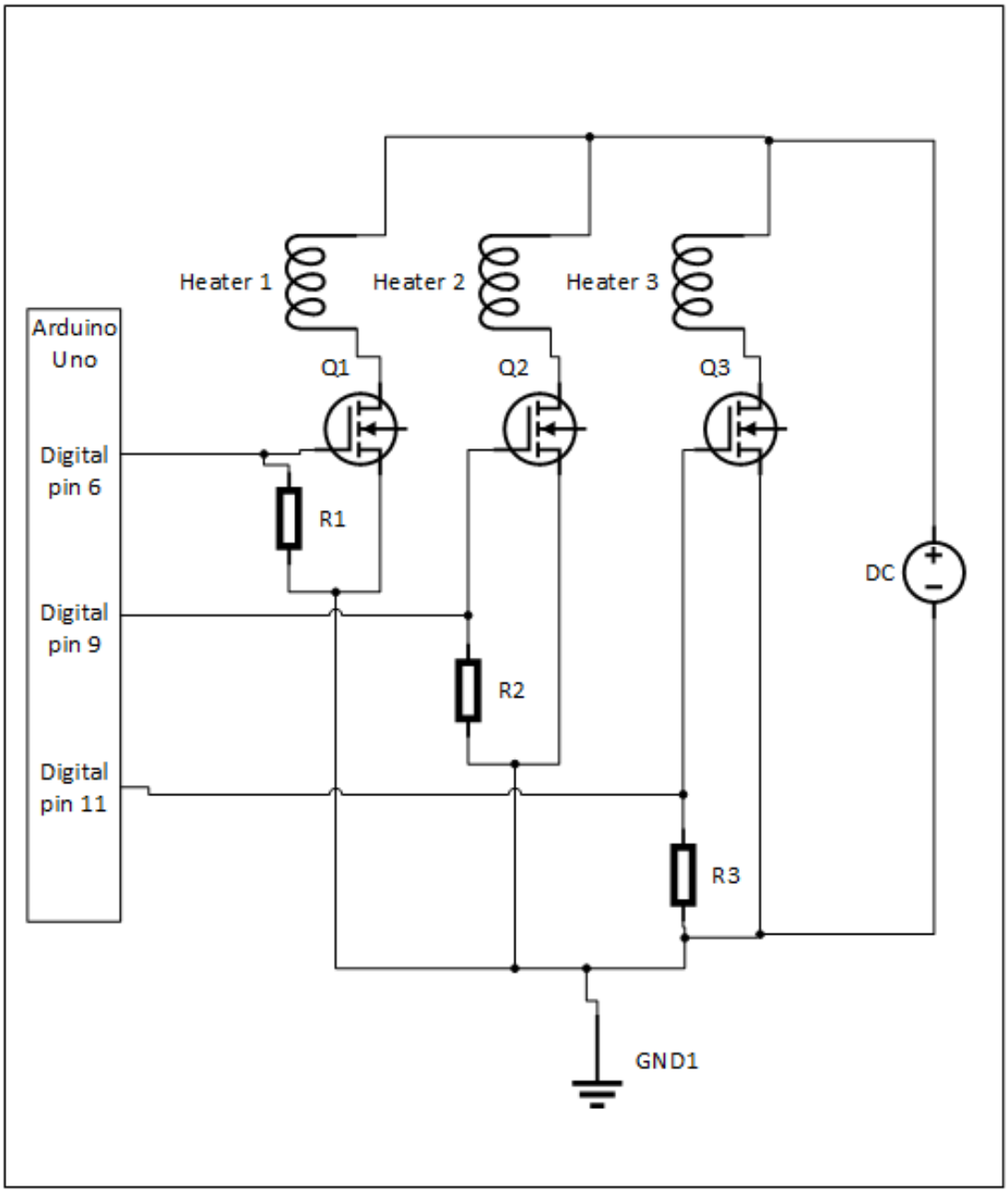

Figure 17. Schematic of the Arduino Proto Shield -circuit used to control powers of the heating elements. The gate voltage, and thus the power directed to the heaters, is controlled with three digital pins in Arduino Uno.[70]

Different powers were used with different pumping speeds to keep the evaporation capability of the heater equal with the volume being pumped. After initial experiments, a linear relationship between heater power, calculated from equation (8) with known voltage and current, and the pumping speed to achieve stable evaporation was found (Fig. 18). The produced gas concentration and evaporation were considered stable when after ten minutes from starting the pumps the signals of ChemPro-channels had stabilized from clean air baseline readings to certain levels and after the pumps were stopped, the channels returned to baseline values within 10 minutes. Using too high powers lead to an unwanted functioning and the produced signals tend to produce error peaks, as the excess power seems to evaporate the solution in an unstable manner inside the PEEK-tube before it reaches the heating element. With too low powers, the solution builds up on the element and the evaporation is not fast enough, thus the provided gas concentration is less than desired.[70]

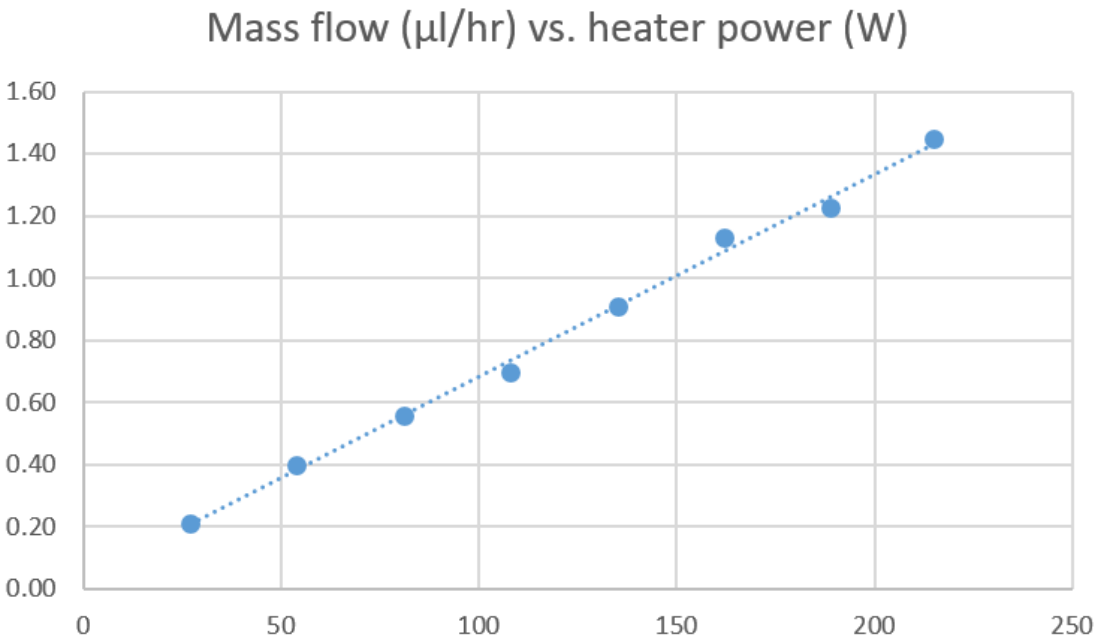

Figure 18. The linear relationship between heater power and pumping speed.

In order to stabilize the temperature conditions, an HTWAT Series silicone rubber heating tape (Omega, USA) was installed to cover the part of the system after the evaporation blocks. Applying external heating achieved a few beneficial things; the time it takes for the system to be clean, meaning that all the residues from the pneumatic tubing and connectors are evaporated, is shorter. Secondly, as vapor pressure is affected by the temperature, keeping the part of the system dealing with the odor flows in as constant temperature as possible ensures that the evaporation capability also stays constant.[70]

Lastly, the varying ceramic heater powers and external temperature changes (which were present in our laboratory environment) do not affect the temperature of the system anymore as much as before applying external heating, which makes the cell temperature more

stable. ChemPro 100i has a built-in heater, which eventually stabilizes the cell temperature somewhere between 30 and 35 °C in our laboratory conditions, depending on the external temperature. With the external rubber heater tape, the cell temperature stabilizes to 35.5-36.5 °C faster and with less variation (Fig. 19). Stable temperature is important to get reliable reading from the IMS-device as changes in temperature affect the signals particularly when detecting molecules that belong to the thermodynamic group and have low PA. If the temperature inside the ionization chamber is not stable, the changing conditions affect the response of detector plates detecting these ions.

The temperature of the whole system was also observed using a FLIR One (FLIR Systems Inc., USA) heat camera. Figure 20 shows that the temperature is stable for the whole part of the olfactometer tubing covered with the heater tape. Only “hot spot” is the adapter connecting the three channels together, but this should not propose a big problem as all the channels go through there so the situation for all the channels is the same. Furthermore, it is advantageous that the adapter, being also a possible source of residues with metallic parts, is heated slightly more for faster cleansing.[70]

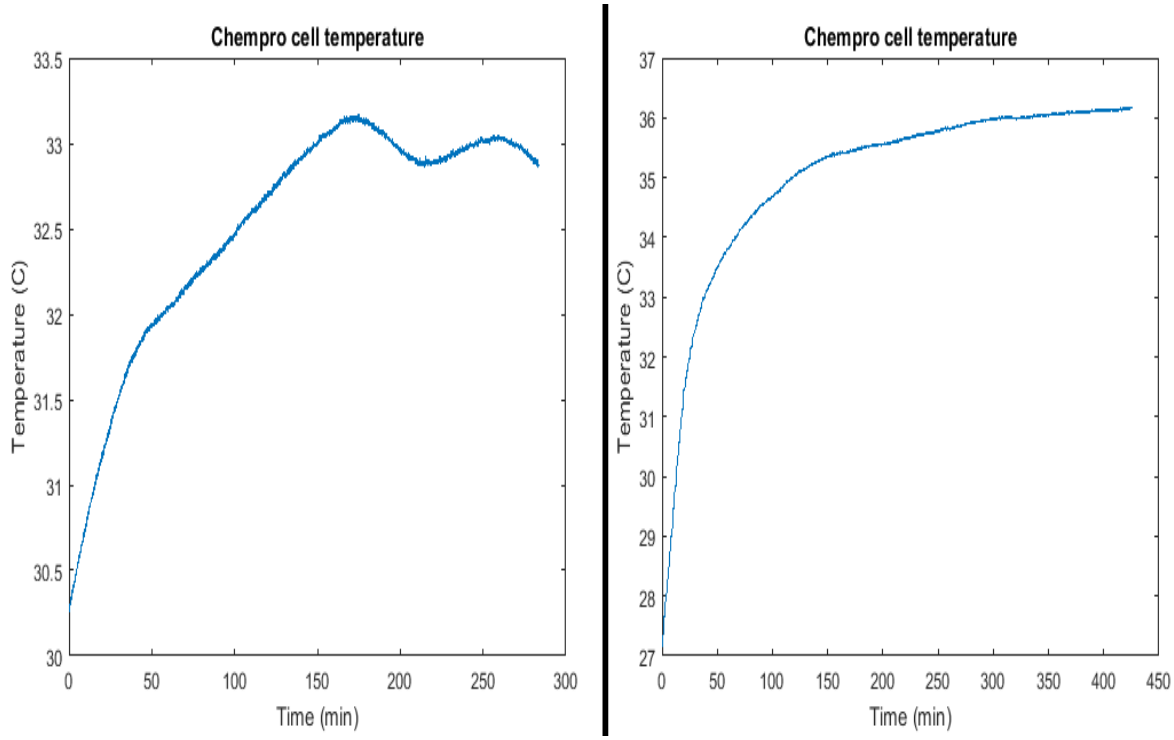

Figure 19. A typical ChemPro 100i ionization cell temperature signal before applying the Omega rope heater (left) and after applying it (right) over a few hours of running the system.

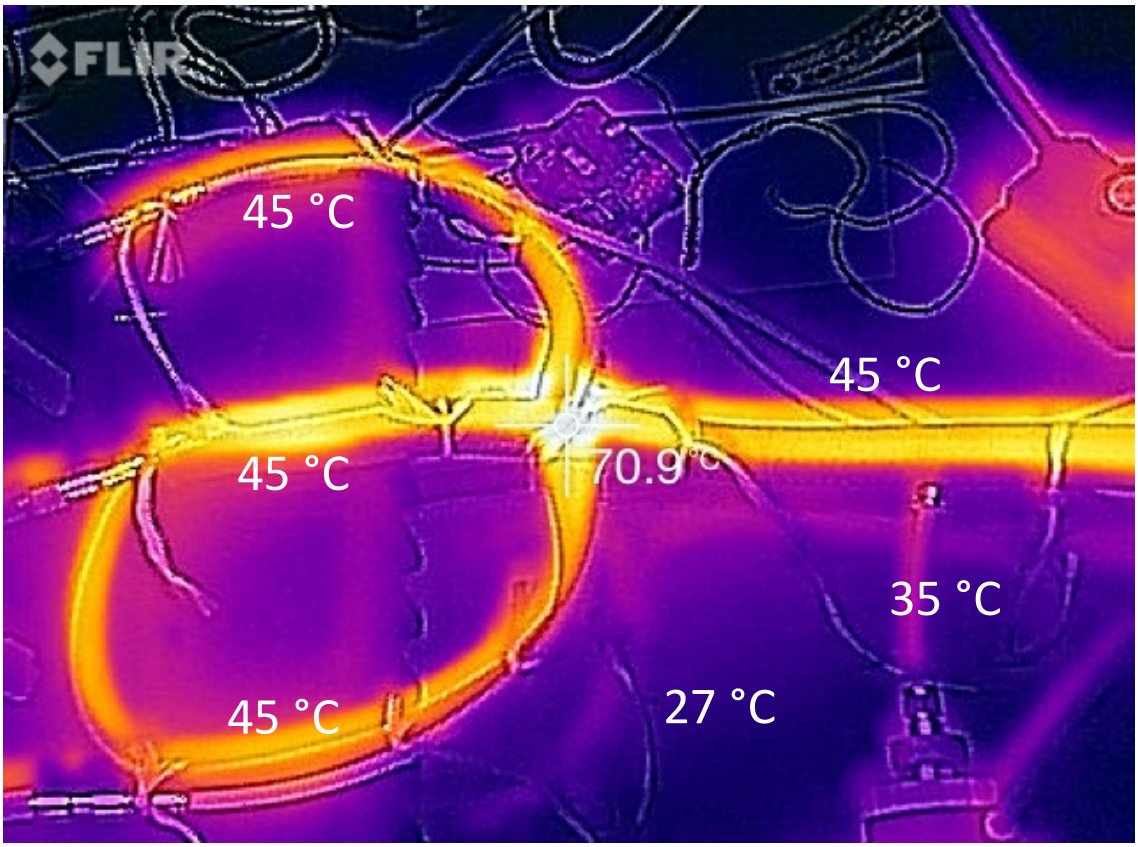

Figure 20. Thermal image of the part of the sample handling system dealing with gas phase odorants. [70]

The measurement data from ChemPro 100i is recorded using software provided by the same manufacturer, Environics. The rest of the system is controlled with Matlab using scripts and functions. The heating elements initially controlled with Arduino terminal can also be controlled in Matlab together with the pumps after installing Arduino hardware -add-on for Matlab.

After the linear relation between heater power and the pumping speed was found, experimental power control was designed. A Matlab function was written to read corresponding pumping speed and gate voltage -pairs and set the voltages on corresponding Arduino pins.

Each concentration corresponds to a pumping speed. The resulting gas mass concentration for each pumping speed is calculated first by calculating the volume of odor component in the solution

$$\boldsymbol{V_o = \frac{mp \cdot \rho_{pg} \cdot V_{tot}}{(1-mp) \cdot \rho_o + mp \cdot \rho_{pg}}}, \qquad (9)$$

where mp is the mass percentage of the odorant in the solution, ρ_{pg} and ρ_o are the densities of the dilutant and odorant, respectively. V_{tot} is the total volume of the solution. As

the values to control the syringe pumps are in the order of $\mu l/hr$, all the volumes used in calculations are given for one hour of operation.[70]

The volume of the dilutant is calculated from

$$\boldsymbol{V_{pg} = V_{tot} - V_o} \qquad (10)$$

With known properties for the carrier gas, the resulting gas mass concentration of the odorant in the output gas flow is calculated from

$$\boldsymbol{ppm_o = \left(\frac{\rho_o \cdot V_o}{\rho_a \cdot V_a + \rho_o \cdot V_o + \rho_{pg} \cdot V_{pg}}\right) 10^{-6}} \qquad (11)$$

where ρ_a and V_a are the density and volume of the carrier gas. As air is used in the presented system as the carrier gas, the numerical values are1.293kg·m^{-3} and 0.324m^3·h^{-1} (= 5.4l·min^{-1}).[70]

There are various limiting factors determining the concentration range able to be produced with our olfactometer. The used syringe pumps have 400-step stepper motors and the flow of the odor solution with the lowest possible pumping speeds produced uneven signals. Our tests revealed pumping speeds of 20 $\mu l/hr$ and lower to be problematic. With low pumping speeds the time constants, namely the stabilization phase, became longer as the system first had to fill up the PEEK tube volume of approximately 6 μl before the odor solution reached the heating element. Long waiting times are especially problematic when considering odor perception testing with human participants. This problem can likely be diminished by implementing an initial pumping phase to the syringe pump. [70]

The upper limit of the concentration range is largely determined by the carrying capacity of the carrier gas. If the gas is saturated, increases in pumping speeds does not produce higher concentrations but the odor components start to condense in the tubing walls. This became a problem when using speeds higher than 220 $\mu l/hr$. When considering the concentration range in logarithmic scale, the range able to be achieved by varying the pumping speeds is approximately one decade. Figure 21 demonstrates the estimated concentrations produced with the olfactometer. As each of the components is diluted with propylene glycol, the “location” of the decade on the ppm scale is determined by mass percent-

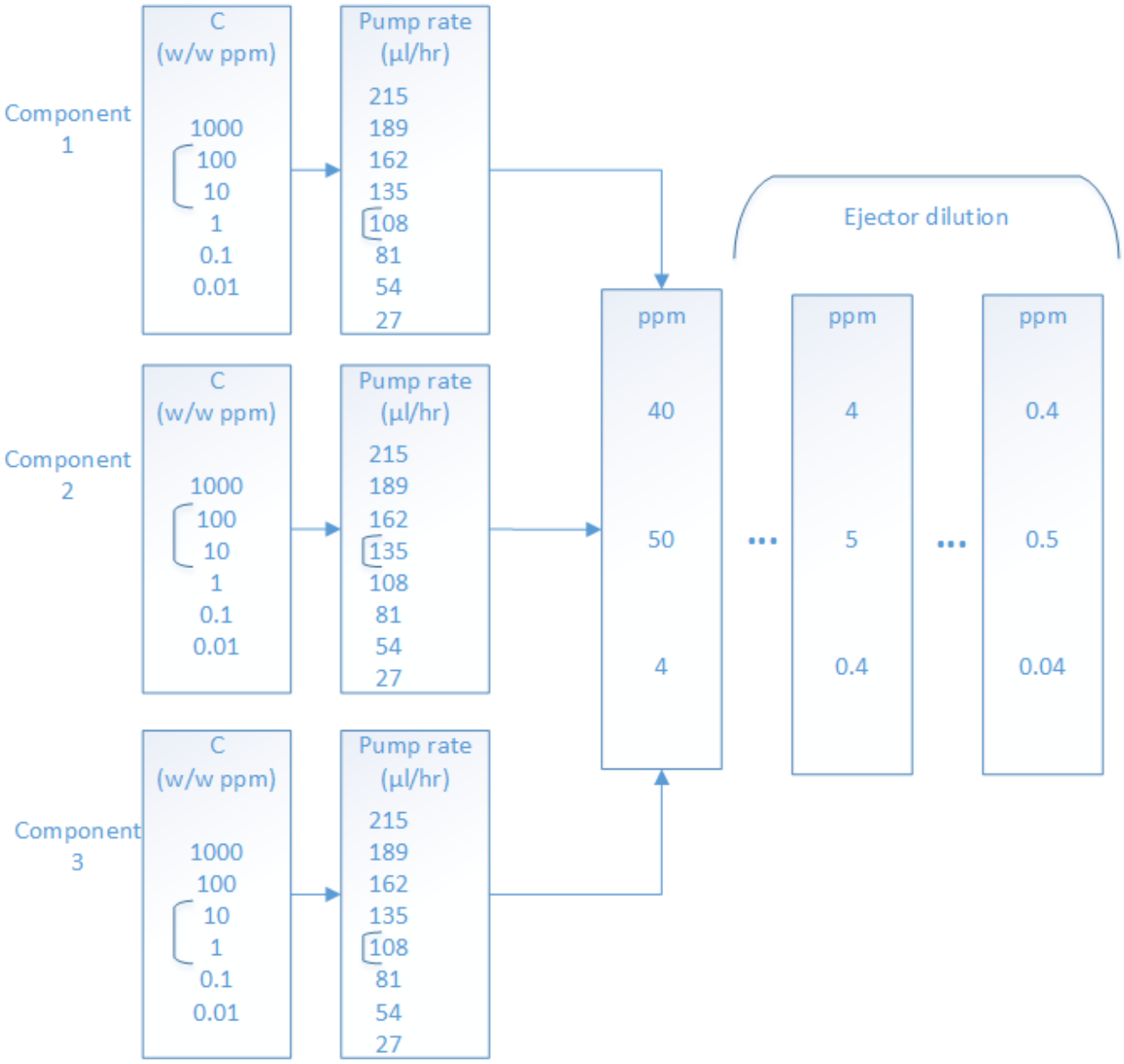

Figure 21. Visualization of determining the theoretical produced gas mass concentrations. In the first stage, the location of the range of gas concentration of the odor component in ppm-scale is determined by the concentration of the selected dilution. In the second stage, the gas mass concentration in the output is determined by the selected pump rate. Thirdly, the set of odorants in the output can be further diluted with additional ejector dilution stage.

age of the odorant in the solution. The selected pump rate determines the mass concentration of the odor component produced in the gas output according to (11). An additional dilution stage can be applied by using an ejector in the output of the system. Dilution with an ejector affects all the components when applied in the output where all the odor components are present. This means that with ejector dilution the interrelation of the concentrations between different components remains the same and the whole mixture of components is diluted in same proportion.[70]

4. MEASUREMENTS & RESULTS

Measurements conducted were firstly done with the motivation to study and verify how well the compact olfactometer works and how well the different odor components with different concentrations can be distinguished from the ChemPro 100i –data. For this purpose, measurements with one, two and all three odor components were carried out. Figure 22 shows signals from the negative ChemPro 100i -channels for two two odor component measurements with BEA and IND with two different concentration pairs.

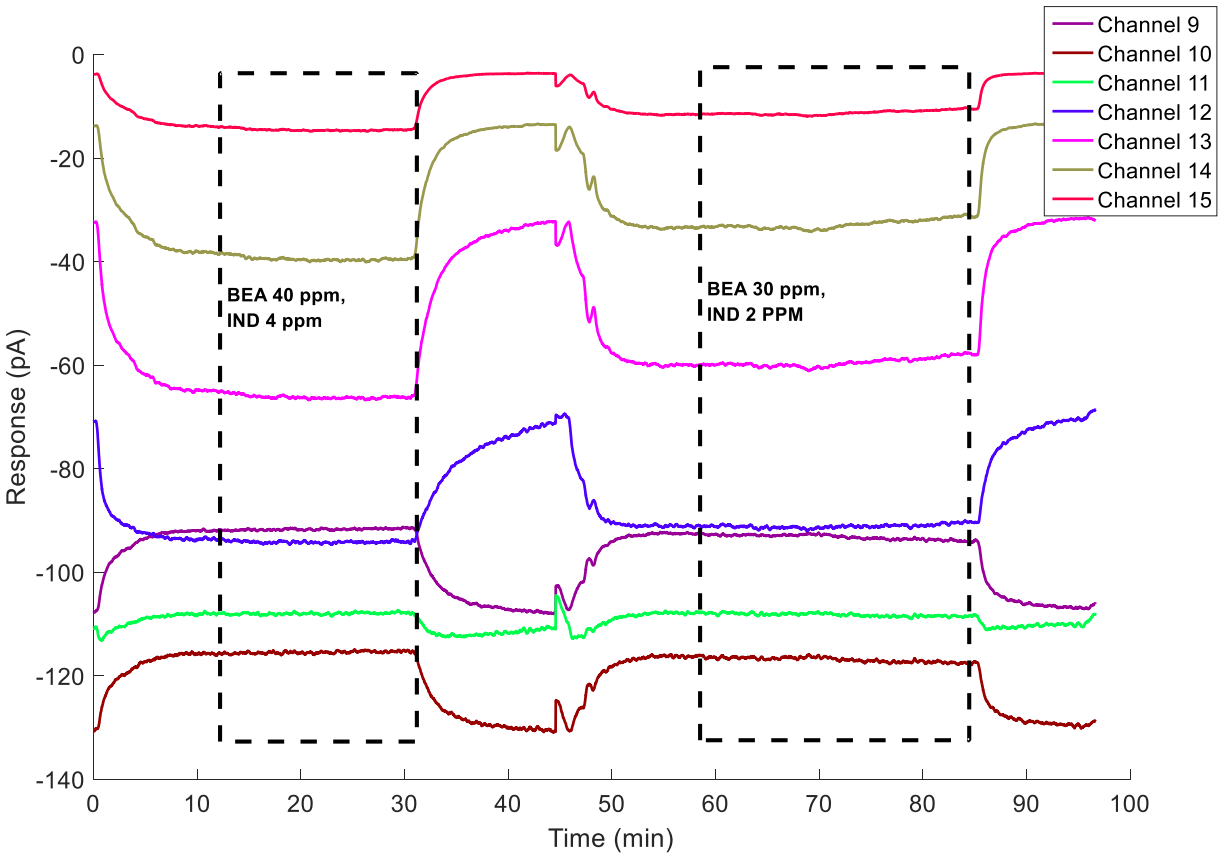

Figure 22. The negative ChemPro 100i-channels for two two odor component measurements

Reading only the signals from different channels does not provide us comprehensive information about the odor components so some other form to represent the data is useful. Sammon mapping is an algorithm for multidimensional scaling, which means that it represents high-dimensional information (14 ChemPro 100i -channels in this case), in a space of lower dimensionality. The mapping, executed in this work using a Matlab script written for this purpose, works by taking 60 data points from each channel over five minutes of measurement data during the stable phase of odor component production and

representing it in lower dimensionality. The number of different measurements can be selected and has no set limit. Even though Sammon mapping is considered a non-linear approach, which means that it is difficult to use for actual classification for odors, it still provides useful information in the interrelation of different datasets and at the very least tells if ChemPro 100i considers given input datasets as identical or if it can distinguish them. For data analysis purposes, a set of 36 two component measurements were conducted with BEA and IND, each having six different concentrations. Based on these measurements, measurements with the three-component synthetic jasmine oil were also conducted. The aim was to produce data with identical concentrations for BEA and IND but now with the addition of CIS as well. Figure 23 shows the signal from a single

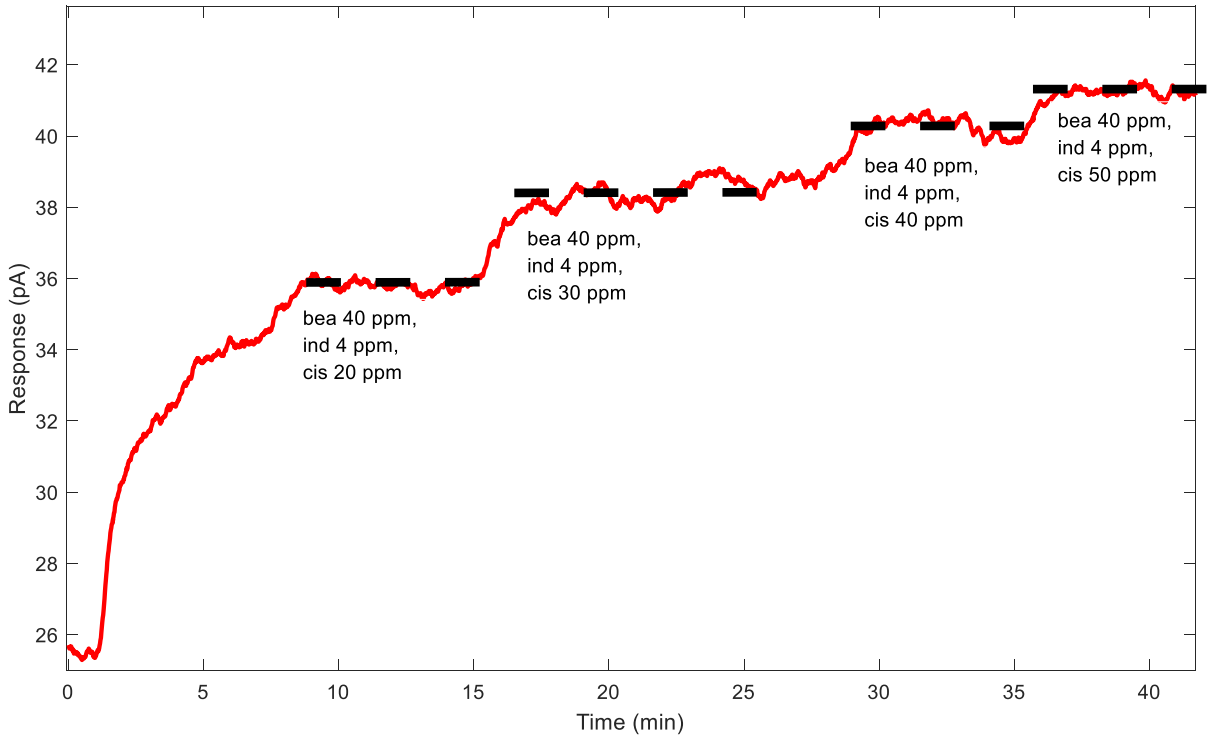

Figure 23. The response of ChemPro 100i channel 6 over a three component measurement cycle with stable concentrations marked with a dashed line.[70]

ChemPro 100i-channel for one measurement cycle. The syringe pumps were programmed to produce continuous, stable pumping from the channels with BEA and IND with a single concentration for the whole duration of cycle. On top of these, the concentration of CIS was increased gradually in 12 minute intervals.[70]

Using Sammon mapping is especially useful when comparing a larger set of inputs. Figure 24 presents a Sammon map for seven different three component measurement data. From there it can be seen that the data sets are distinguished from each other with only little overlapping. When considering the plotted datasets in pairs where two components (BEA and IND, or BEA and CIS) have the same concentration, increasing the third component moves the dataset consistently in the sammon map in different direction. This gives us more confidence in that the perceived differences in the signals are in fact due to the odor components and not the diluent PG.[70]

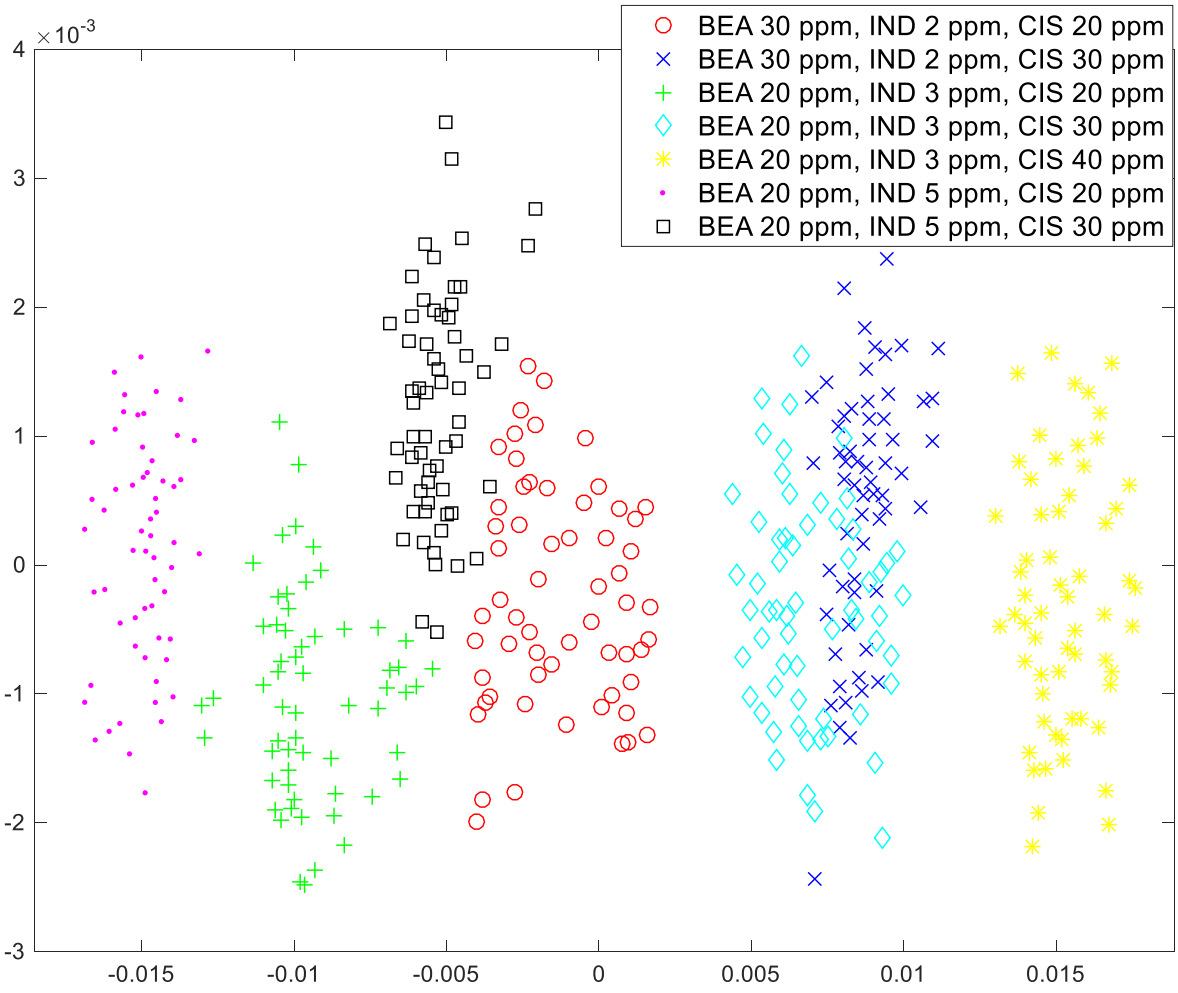

Figure 24. Sammon map for seven three odor component measurements with different concentrations[70]

For human perception testing, the introduced olfactometer was also used in prototype setup to conduct measurements with more complex solutions in the syringes; diluted jasmine oil and synthetic jasmine oil with two components (BEA and CIS, i.e. binary scent) and three (i.e.tertiary scent) components (BEA,CIS and IND). Each of these solutions was presented using only one channel, so in this case the relative proportions between the components was not possible to be varied. The relative proportions of odor components

in synthetic jasmine oils were calculated to be in theory the same as detected in the real jasmine oil in MS measurements.[70]

To study whether participants of the human perception testing were able to distinguish synthetic jasmines from real jasmine oil, a same – different task as used. Odors were presented sequentially to the participant. The task was to indicate whether they were the same or different. All the possible combinations of odors were used so that the total of odor pairs presented was nine. The collected data was coded by 1 (same) and 0 (different). A chi-squared test showed a statistical difference from expected frequency when comparing real jasmine oil and binary synthetic jasmine (x^2=6.4, $p < 0.05$ both when real jasmine was presented first and when binary synthetic jasmine was presented first). These mean differences showed that the two odors were correctly identified as different. Other tests were not statistically significant.[70] The measurement data from this experiment was also collected with ChemPro 100i and the sammon map for the three stimuli used is shown in Figure 25, which shows similar identification as with human perception.

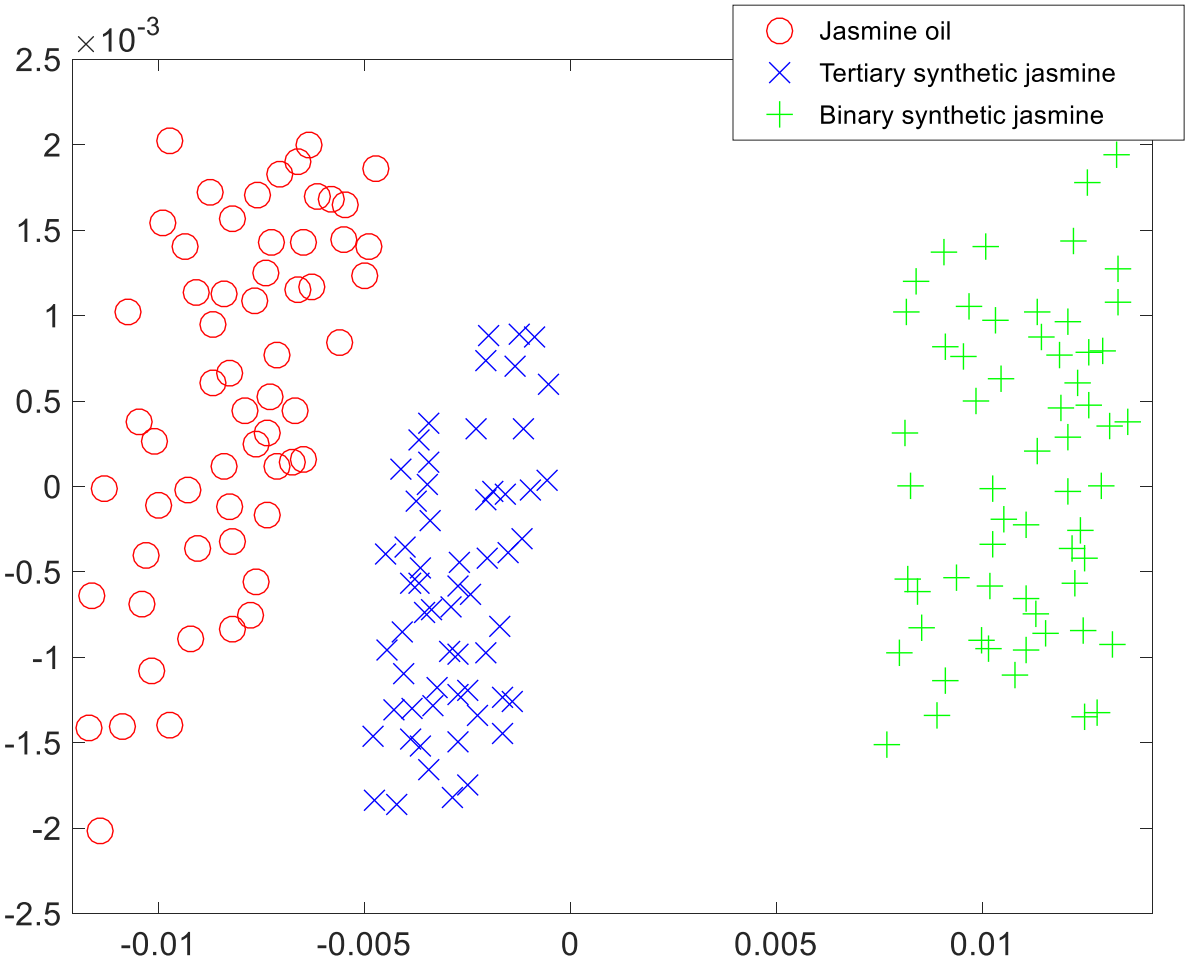

Figure 25. Sammon map for ChemPro 100i data produced using jasmine oil and two versions of synthetic jasmine scent[70]

In collaboration with Tampere University of Applied Sciences (TAMK), samples from the olfactometer was also collected and analyzed with GC-MS device (Agilent Technologies 6890N&5973). Figure 26 shows the setup for collecting the samples using AirChek

Figure 26. The setup for collecting adsorption tube samples for GC-MS analysis using Aircheck 3000.

3000-device (SKC Ltd, UK). The device sucks the air with a set flow rate and for a set time from the output airflow of the olfactometer through an adsorption tube. Two samples were analyzed with GC-MS, one when producing only one component, BEA, at a constant concentration and one when producing BEA and CIS. The GC-MS spectrum for the sample collected over 100 minutes of system producing ideally only BEA (and PG) is seen on Figure 27 showing the identified peaks. The compounds for different peaks were identified from existing library and identified as BEA, CIS and PG. The existence of CIS-peak when the syringe pumps were only pumping BEA tells us that the evaporation units do not cleanse as well as intended but some amount of residues are present. These residues still seem to be below the human detection threshold as they were not sensed in the output of the system while collecting the samples.[70]

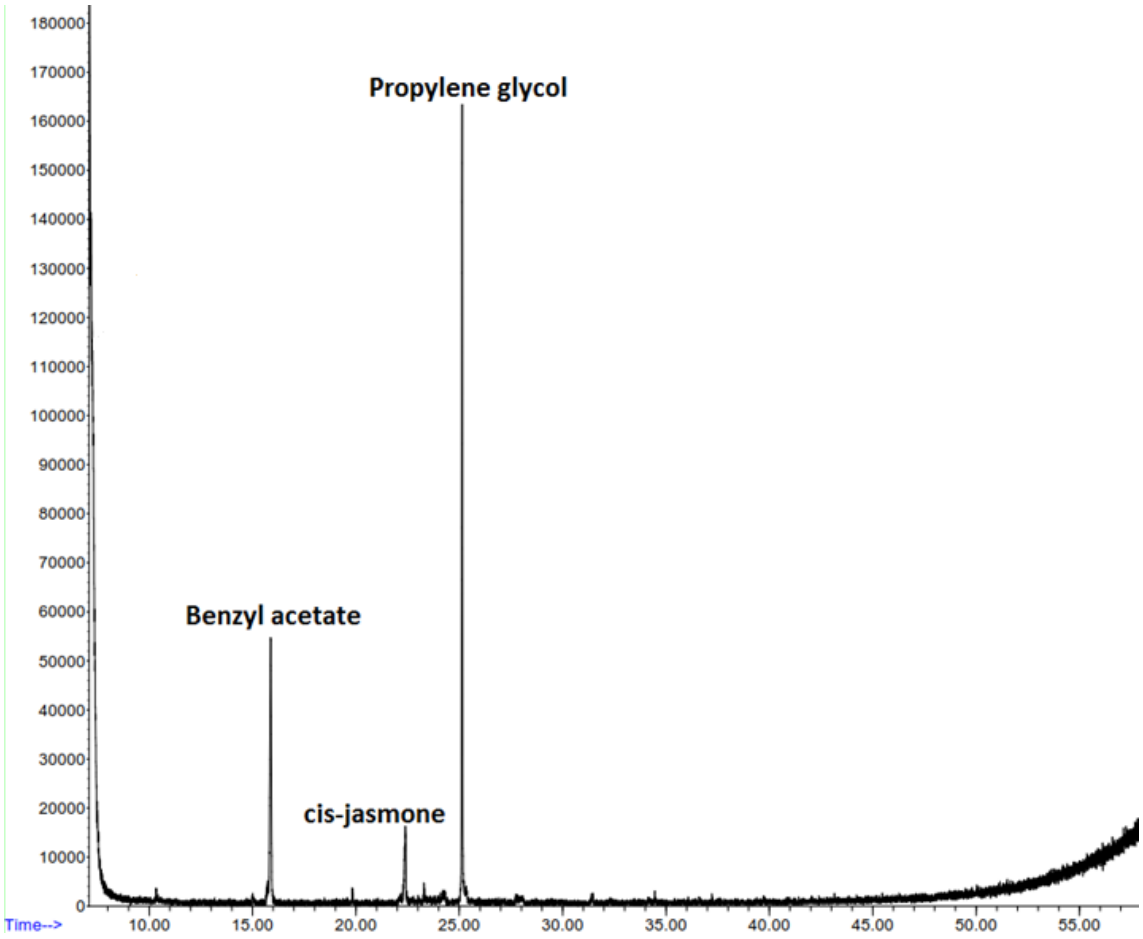

Figure 27. GC-MS spectrum for a sample produced with the presented olfactometer showing and identifying the most visible peaks.

5. DISCUSSION

The achieved concentration range with the introduced olfactometer is limited by many factors. In the lower limit of the range, the 400-step stepper motors proved to be the main limiting factor as when using pumping speeds of 20 $\mu l/hr$ and lower, flow of the odor solution is not constant enough to provide stable signal and gas concentrations. This problem can likely be diminished by using syringes with smaller diameters and by implementing an initial pumping phase to the syringe pump in order to fill the 6µl volume of the PEEK tube before the actual measurement starts.

In the upper limit of the concentration range, the main limiting factor is the carrying capacity of the carrier gas. If the gas is saturated, increases in pumping speeds do not produce higher concentrations but the gaseous components start to condense in the tubing walls. This was reduced with the external rubber tape heater by heating the tubings that are in contact with the evaporated odor components. Heating the system in higher temperature could further improve the range, but would also introduce new problems with low heat resistance of the pneumatic adapters containing nitrile rubber O-rings. Also, considering human perception testing, the temperature of the gas can affect the perception of the odor and using heavily heated gases in temperature higher than body temperature is not ideal.

The GC-MS -results revealed that the cleansing of the evaporation units is not as good as thought. Even though the concentrations of the odor components in the gas flow seem to drop below the human detection threshold, the sensitive GC-MS was able to distinguish peaks in the collected sample for the unused odor component when only one should be present. Further analysis with additional GC-MS samples is needed to get information on the actual produced concentrations to verify how well the calculated theoretical values represent actual concentrations in the olfactometer output.

Additional improvements for the evaporation units are needed in order to get rid of residues from unused channels. One solution could be installing additional programmable valves to each of the channels to control the airflow in a way that only the channels producing odor components would have airflow through the evaporation units in the output of the system and the rest of the channels would be either closed or the airflow directed directly to the activated carbon filter. Also, possible wear down regarding most importantly the ceramic heating elements must be considered when assessing the functioning of the system in long term.

A duplicate of the olfactometer was also built for the use of research group for Emotions, Sociality and Computing in University of Tampere (UTA). One of their goals is to use the olfactometer in human perception tests by combining virtual reality and odor stimulus.

The ideas for future use of the olfactometer deal with introducing new odor components to produce other synthetic odors in addition to synthetic jasmine scent. Preliminary tests with components such as limonene and vanillin to produce synthetic scents of lemon and vanilla have successfully been performed. Other possible synthesizable odors include various fruits, mushrooms, foodstuff, and more abstract smells like forest.

6. CONCLUSIONS

The presented olfactometer is able to produce gas flow with constant, stable gas concentrations of the selected odor components. When producing single odor components, the achieved concentration range was approximately one decade. With more components produced at the same time, the carrier gas started to saturate at high concentrations and the achieved range for each component was approximately half a decade when producing three odor components at the same time. ChemPro 100i proved to be a valuable reference tool to analyze how stable the concentrations of the produced odor components are. Analysis with the data from the conducted measurements suggests that it is possible to distinguish measurements with different concentration sets. Although more work to verify the genuine gas concentrations of the produced odor components in the olfactometer output is needed, the data has proven so far to be reproducible and it is useful for further data analysis.

Human perception testing with the olfactometer also proved to be feasible, although relatively long time constants to reach the stable gas concentration in the output of the olfactometer and between changing concentrations make it somewhat problematic and careful planning regarding each experiment setup is needed. The olfactometer still provides a functional platform for various olfactory-related human perception tests.

REFERENCES

[1] S. Sankaran, L. R. Khot, and S. Panigrahi, “Biology and applications of olfactory sensing system : A review,” *Sensors Actuators B. Chem.*, vol. 171–172, pp. 1–17, 2012.

[2] C. Spence, “The multisensory perception of flavour,” *Psychologist*, vol. 23, no. 9, pp. 720–723, 2010.

[3] P. Rozin, “‘ Taste-smell confusions ’ and the duality of the olfactory sense,” vol. 31, no. 4, pp. 397–401, 1982.

[4] I. Croy *et al.*, “Olfaction as a marker for depression in humans,” *J. Affect. Disord.*, vol. 160, pp. 80–86, 2014.

[5] B. M. Kolakowski, P. A. D’Agostino, C. Chenier, and Z. Mester, “Analysis of chemical warfare agents in food products by atmospheric pressure ionization-high field asymmetric waveform ion mobility spectrometry-mass spectrometry,” *Anal. Chem.*, vol. 79, no. 21, pp. 8257–8265, 2007.

[6] D. S. Giordani, H. F. Castro, P. C. Oliveira, and A. F. Siqueira, “Biodiesel characterization using electronic nose and artificial neural network,” no. September, pp. 16–20, 2007.

[7] X. F. X. Fang, X. G. X. Guo, H. S. H. Shi, and Q. C. Q. Cai, “Determination of Ammonia Nitrogen in Wastewater Using Electronic Nose,” *Bioinforma. Biomed. Eng. (iCBBE), 2010 4th Int. Conf.*, pp. 1–4, 2010.

[8] S. Labreche, S. Bazzo, S. Cade, and E. Chanie, “Shelf life determination by electronic nose: Application to milk,” *Sensors Actuators, B Chem.*, vol. 106, no. 1 SPEC. ISS., pp. 199–206, 2005.

[9] S. Benedetti, N. Sinelli, S. Buratti, and M. Riva, “Shelf Life of Crescenza Cheese as Measured by Electronic Nose,” *J. Dairy Sci.*, vol. 88, no. 9, pp. 3044–3051, 2005.

[10] E. Schaller, J. O. Bosset, and F. Escher, “‘Electronic Noses’ and Their Application to Food,” *Leb. und-Technologie*, vol. 31, no. 4, pp. 305–316, 1998.

[11] S. Firestein, “How the olfactory system makes sense of scents,” vol. 413, no. September, pp. 211–218, 2001.

[12] A. D. Wilson and M. Baietto, “Applications and Advances in Electronic-Nose Technologies,” *Sensors*, vol. 9, no. 1, pp. 5099–5148, 2009.

[13] R. Schmidt and W. S. Cain, “Making scents: dynamic olfactometry for threshold measurement.,” *Chem. Senses*, vol. 35, no. 2, pp. 109–20, Feb. 2010.

[14] J. U. Sommer *et al.*, “A mobile olfactometer for fMRI-studies,” *J. Neurosci. Methods*, vol. 209, no. 1, pp. 189–194, 2012.

[15] J. Gutiérrez and M. C. Horrillo, “Advances in artificial olfaction: Sensors and applications,” *Talanta*, vol. 124, pp. 95–105, 2014.

[16] “A Technical Guide for Static Headspace Analysis Using GC.” Restek Ltd.

[17] J. N. Lundström, A. R. Gordon, E. C. Alden, S. Boesveldt, and J. Albrecht, “Methods for building an inexpensive computer-controlled olfactometer for temporally-precise experiments,” *Int. J. Psychophysiol.*, vol. 78, no. 2, pp. 179–189, Nov. 2010.

[18] R. Fernandez-Maestre, “ION MOBILITY SPECTROMETRY : HISTORY , CHARACTERISTICS AND APPLICATIONS,” pp. 467–479, 2012.

[19] L. Sela and N. Sobel, “Human olfaction : a constant state of change-blindness,” pp. 13–29, 2010.

[20] R. Summary, “Poor human olfaction is a 19th-century myth,” vol. 7263, 2017.

[21] H. Breer, “Sense of smell : recognition and transduction of olfactory signals,” pp. 113–116, 2003.

[22] T. Thomas-Danguin *et al.*, “The perception of odor objects in everyday life: a review on the processing of odor mixtures,” *Front. Psychol.*, vol. 5, no. June, pp. 1–18, 2014.

[23] B. Auffarth, “Understanding smell — The olfactory stimulus problem,” *Neurosci. Biobehav. Rev.*, vol. 37, no. 8, pp. 1667–1679, 2013.

[24] E. Guichard, *Flavour : from food to perception*. Chichester, West Sussex Hoboken, NJ: John Wiley & Sons Inc, 2017.

[25] S. B. Olsson, “Odor objects in a complex world,” vol. 3, no. Suppl 1, p. 2014, 2014.

[26] K.-T. Tang, S.-W. Chiu, C.-H. Pan, H.-Y. Hsieh, Y.-S. Liang, and S.-C. Liu, “Development of a Portable Electronic Nose System for the Detection and Classification of Fruity Odors,” *Sensors*, 2010.

[27] S. Omatu, “Odor classification by neural networks,” *Proc. 2013 IEEE 7th Int. Conf. Intell. Data Acquis. Adv. Comput. Syst. IDAACS 2013*, vol. 1, no. September, pp. 309–314, 2013.

[28] R. Brugarolas, T. Agcayazi, S. Yuschak, D. L. Roberts, B. L. Sherman, and A. Bozkurt, “Towards a wearable system for continuous monitoring of sniffing and panting in dogs,” pp. 292–295, 2016.

[29] M. E. Staymates *et al.*, “Biomimetic Sniffing Improves the Detection Performance of a 3D Printed Nose of a Dog and a Commercial Trace Vapor Detector,” *Nat. Publ. Gr.*, no. October, pp. 1–10, 2016.

[30] B. A. Craven, E. G. Paterson, and G. S. Settles, “The fluid dynamics of canine olfaction : unique nasal airflow patterns as an explanation of macrosmia,” no.

December 2009, pp. 933–943, 2010.

[31] A. Ulanowska, T. Ligor, M. Michel, B. Buszewski, Ł. I Niekonwencjonalne, and M. Poszukiwania, *Hyphenated and unconventional methods for searching volatile cancer biomarkers*, vol. 17. 2010.

[32] J. Susaya, K.-H. Kim, J. W. Cho, and D. Parker, "The use of permeation tube device and the development of empirical formula for accurate permeation rate," *J. Chromatogr. A*, vol. 1218, no. 52, pp. 9328–9335, 2011.

[33] P. J. Moate, M. H. Deighton, B. E. Ribaux, M. C. Hannah, W. J. Wales, and S. R. O. Williams, "Michaelis–Menten kinetics predict the rate of SF6 release from permeation tubes used to estimate methane emissions from ruminants," *Anim. Feed Sci. Technol.*, vol. 200, pp. 47–56, 2015.

[34] P. Rahimi and C. A. Ward, "Kinetics of Evaporation Statistical Rate Theory Approach," *Int. J. Thermodyn.*, vol. 8, no. 1, pp. 1–14, 2005.

[35] B. Magin and E. Randall, "Review of Literature on Evaporation Suppression," 1960.

[36] A. S. Sonmezdag, H. Kelebek, and S. Serkan, "Identification of Aroma Compounds of Lamiaceae Species in Turkey Using the Purge and," 2017.

[37] J. Omar, M. Olivares, I. Alonso, A. Vallejo, O. Aizpurua-Olaizola, and N. Etxebarria, "Quantitative Analysis of Bioactive Compounds from Aromatic Plants by Means of Dynamic Headspace Extraction and Multiple Headspace Extraction-Gas Chromatography-Mass Spectrometry," *J. Food Sci.*, vol. 81, no. 4, pp. C867--C873, 2016.

[38] M. Huang, H. Chen, S. Fu, and W. Ding, "Determination of volatile N - nitrosamines in meat products by microwave-assisted extraction coupled with dispersive micro solid-phase extraction and gas chromatography – Chemical ionisation mass spectrometry," *Food Chem.*, vol. 138, no. 1, pp. 227–233, 2013.

[39] K. Hashimoto and T. Nakamoto, "Tiny Olfactory Display Using Surface Acoustic Wave Device and Micropumps for," vol. 16, no. 12, pp. 4974–4980, 2016.

[40] D. E. Williams, "Semiconducting oxides as gas-sensitive resistors," vol. 57, no. January, pp. 1–16, 1999.

[41] N. Barsan, D. Koziej, and U. Weimar, "Metal oxide-based gas sensor research : How to ?," vol. 121, pp. 18–35, 2007.

[42] H. Meixner and U. Lampe, "Metal oxide sensors," 1996.

[43] T. Shigemori, "Gas Sensors Status and Future Trends for Safety Applications," pp. 49–51, 2012.

[44] Sensirion, "Preliminary Datasheet SGP30," no. July. Sensirion, pp. 1–15, 2017.

[45] U. Lange, N. V Roznyatovskaya, and V. M. Mirsky, "Conducting polymers in

chemical sensors and arrays," vol. 4, pp. 1–26, 2008.

[46] A. L. P. S. Bailey, A. M. Pisanelli, and K. C. Persaud, "Development of conducting polymer sensor arrays for wound monitoring," vol. 131, pp. 5–9, 2008.

[47] F. Gu, L. Zhang, X. Yin, and L. Tong, "Polymer Single-Nanowire Optical Sensors 2008," 2008.

[48] M. Nakhleh *et al.*, "Diagnosis and Classi fi cation of 17 Diseases from 1404 Subjects via Pattern Analysis of Exhaled Molecules," 2017.

[49] M. Huotari, "Odour Sensing by Insect Olfactory receptor neurons: Measurements of Odours based on Action Potential analysis," 2004.

[50] M. Hassan and A. Bermak, "Hardware Friendly Gas Identification With the Array of Gas Sensors," vol. 16, no. 14, pp. 5776–5784, 2016.

[51] K. H. Esbensen, K. I. M. Esbensen, and P. Geladi, "Principal Component Analysis," vol. 7439, no. January 2014, 1987.

[52] F. Amato, A. López, E. M. Peña-méndez, P. Vaňhara, and A. Hampl, "Artificial neural networks in medical diagnosis," pp. 47–58, 2013.

[53] A. Krogh, "What are artificial neural networks ?," vol. 26, no. 2, pp. 195–198, 2008.

[54] J. W. Sammon, "Nonlinear Mapping Structure Analysis," vol. C, no. 5, 1969.

[55] R. M. Page and P. Huggenberger, "Multivariate Analysis of Groundwater-Quality Time-Series Using Self-organizing Maps and Sammon ' s Mapping," pp. 3957–3970, 2015.

[56] S. Bharitkar and C. Kyriakakis, "Visualization of Multiple Listener Room Acoustic Equalization With the Sammon Map," vol. 15, no. 2, pp. 542–551, 2007.

[57] G. A. Eiceman, *Ion mobility spectrometry*, 3rd ed. CRC Press, 2013.

[58] C. Poole, *Handbook of methods and instrumentation in separation science*. Elsevier, 2009.

[59] K. E. Swearingen and R. L. Moritz, "High Field Asymmetric Waveform Ion Mobility Spectrometry (FAIMS) for Mass Spectrometry-Based Proteomics," vol. 9, no. 5, pp. 505–517, 2016.

[60] J. Puton and M. Nousiainen, "Ion mobility spectrometers with doped gases," vol. 76, pp. 978–987, 2008.

[61] S. G. Lias, *Gas-phase ion and neutral thermochemistry*. Published by the American Chemical Society and the American Institute of Physics for the National Bureau of Standards, 1988.

[62] J. Li *et al.*, "Using Field Asymmetric Ion Mobility Spectrometry for Odor

Assessment of Automobile Interior Components," vol. 16, no. 14, pp. 5747–5756, 2016.

[63] R. M. Räsänen, M. Håkansson, and M. Viljanen, "Differentiation of air samples with and without microbial volatile organic compounds by aspiration ion mobility spectrometry and semiconductor sensors," *Build. Environ.*, vol. 45, no. 10, pp. 2184–2191, 2010.

[64] P. Mochalski, J. Rudnicka, and A. Agapiou, "Near real-time VOCs analysis using an aspiration ion mobility spectrometer Near real-time VOCs analysis using an aspiration ion mobility spectrometer," no. March, 2013.

[65] R. Huo, "The trapped human experiment," *J. Breath Res.*, vol. 5, no. 4, 2011.

[66] K. L. Busch, "Ion mobility spectrometry: solo or coupled to mass spectrometry.(Mass Spectrometry Forum)," *Spectroscopy*, vol. 28, no. 11, p. 12(4).

[67] "An Introduction to Ion Mobility Spectrometry with UltraFAIMS." Owlstone Nanotech Inc.

[68] R. W. Purves and R. Guevremont, "Electrospray Ionization High-Field Asymmetric Waveform Ion Mobility Spectrometry - Mass Spectrometry," vol. 71, no. 13, pp. 2346–2357, 1999.

[69] R. J. Lewis, Ed., *Hawley's Condensed Chemical Dictionary*. Hoboken, NJ, USA: John Wiley & Sons, Inc., 2007.

[70] V. Nieminen, M. Karjalainen, A. Kontunen, K. Salminen, and J. Rantala, "A compact olfactometer for IMS measurements and testing human perception," Tampere, 2017.

[71] R. Cumeras, E. Figueras, C. E. Davis, J. I. Baumbach, and I. Gràcia, "Review on Ion Mobility Spectrometry. Part 1: current instrumentation," *Analyst*, vol. 140, no. 5, pp. 1376–1390, 2015.